INTRODUCTION

Electrical discharges in many gases and vapours contain plasma regions made up of electrons and positive ions in approximately equal numbers, in addition to the neutral atoms and molecules of the gas. Such discharge plasmas are termed "electropositive" or "non-attaching". In these cases quasineutrality is ensured by the electron concentration (n_e) and positive ion concentration (n_+) being much greater than $\left|n_+ - n_e\right|$.

A separate class of electrical discharges, is that in which the charged species include negative ions in addition to positive ions and electrons. These electron-attaching plasmas are termed "electronegative" if appreciable concentrations of negative ions are capable of being formed. Under these circumstances, quasineutrality is determined by the condition $n_+ \doteqdot n_e + n_-$, where n_- is the negative ion concentration. In strongly electronegative plasmas, $n_+ \doteqdot n_-$ and $n_\pm \gg n_e$.

The behaviour of electrical discharges in electronegative gases is significantly affected by the formation and destruction of negative ions. Not surprisingly, discharges (especially glows) in these gases appear different in several ways from those in non-attaching gases.

Weakly attaching gases include O_2, CO_2 and NO_2, whilst the halogens, $CC\ell_4$, $CC\ell_2F_2$, C_2F_6 and SF_6 amongst others, are strongly electronegative. Over recent years, a considerable degree of attention has been directed towards an understanding of the properties of electrical discharges in these and other electronegative gases. Steady-state glow discharges and transient afterglow plasmas, for example, have been studied in attaching gases, including oxygen and iodine vapour. Such studies have provided data on the basic collision processes of attachment and detachment, and in oxygen for example, this information has helped to account for the formation and properties of the various layers of the earth's upper atmosphere (ionosphere). The halogen-containing compounds have been the subject of investigation, on account of their

high dielectric strength and flame-inhibiting properties. Of these, sulphur hexafluoride (SF_6) has proved to be of exceptional interest, with the electrical properties of this gas and of mixtures containing it, being the subject of considerable experimental and theoretical study.

Experimental work with SF_6 has been focussed primarily on: (i) breakdown and arc processes, because of the widespread use of SF_6 and SF_6-mixtures as insulating and circuit-breaker media, and (ii) the role played by SF_6 in various types of gas laser: for example, in boosting the overall power output; and in producing fluorine for rare gas-halide lasers. Many of the special effects produced in SF_6 in both (i) and (ii) arise from the high electron attachment rate which occurs in discharges through this gas. The interest in the different applications of SF_6 has led to considerable theoretical and experimental work on the fundamental processes which occur in the gas. Consequently, data are now available to varying extents on drift, diffusion, dissociation, ionization, attachment, detachment, charge-transfer and other processes in SF_6.

Despite the interest in SF_6, little work has yet been done on the properties of steady-state glows and on spark discharges in this gas.

The aim of the present thesis is to describe the growth and development of the low pressure SF_6 spark, and to account for certain phenomena associated with some of the spark phases in terms of electron attachment and detachment. The SF_6 spark has presently been studied at low pressure ($\sim$ 1 Torr) partly because time-resolved diagnostic techniques can be more easily applied than at high pressures ($\sim$ 760 Torr). This is because the time-scale of events associated with spark phenomena is relatively longer at low pressures (μs/ms) than at high pressures (ns).

CHAPTER 1

LITERATURE REVIEW

1.1 SPARK DEVELOPMENT IN NON-ATTACHING GASES

The electrical breakdown of a spark gap is characterised by the rapid transition of the gas medium from a poor electrical conductor with a resistivity of some 10^{14} ohm-m to a relatively good conductor with a resistivity dependent on the specific discharge conditions. The resistivity is reduced by several orders of magnitude, becoming typically about 10^{3} ohm-m in a glow discharge. The potential difference required to produce the transition is called the static breakdown, or sparking potential, V_s, which in general depends on the nature and pressure of the gas, the spark gap length and geometry, and the material and state of the electrodes.

Over the past century, numerous researchers have investigated the breakdown potentials of numerous gases in uniform and non-uniform field gaps for varying gap widths and gas pressures. Mechanisms of breakdown for various specified conditions have been determined by combining experimental observations and theoretical predictions obtained from basic data on atomic and molecular collision processes. Furthermore, these basic collision processes have been used to account for the spatial and temporal growth of ionization, from the one or more electrons which must always be present to initiate breakdown, to the final form of discharge. The actual sequence of events occurring during the development of a spark discharge depends on specific parameters such as those already mentioned above which control the sparking potential, together with the percentage overvoltage applied to the gap and the rate at which energy is supplied to the gap. The percentage overvoltage ΔV, is defined as

$$\Delta V = \frac{100(V - V_s)}{V_s} \qquad (1.1a)$$

where V is the applied voltage and V_s is the static breakdown potential. Marked visual differences exist between the various phases of development in low ($\sim$ 1%) and highly ($\gtrsim$ 15%) overvolted gaps. These differences occur because at low overvoltages, both primary and a number of secondary

avalanches contribute to the growth of current according to the Townsend breakdown mechanism (Meek and Craggs, 1978), whereas, at very high over-voltages, high amplification can be produced in the very first avalanche. In the latter case, current growth proceeds by the so-called "streamer" mechanism, for which the space-charge field in the vicinity of the primary avalanche head becomes of the same order as the applied field. For this to be the case, it is believed that the number of charge carriers in the avalanche head must be between 10^8 and 10^9 (Raether, 1939; Loeb and Meek, 1940, Raether, 1940). Under such conditions, rapidly developing filamentary luminous channels or "streamers" propagate across the gap at speeds often in excess of the electron drift velocities (i.e. $> 10^7$ cms^{-1}) and hence in times less than the electron transit time. The formation of these streamers in gas discharges occurs mainly at high pressures. At low pressures ($\lesssim$ 10 Torr), the probability of their development is extremely low (Raether, 1964).

In the past, some workers have attempted to identify the mechanism of breakdown as being either of the Townsend or the streamer type, from a study of the form of voltage collapse that occurs across the discharge gap. In general, there are two basic forms of voltage decay that can occur. These can be referred to as the "stepped -" and the "chopped -" modes of collapse. The stepped form is associated with the transition after breakdown, to a diffuse glow phase and then later to a filamentary arc phase. The chopped form of collapse on the other hand, represents a sudden transition at breakdown to the arc mode without the formation of an intermediate glow phase. The stepwise collapse has long been observed to occur in air (Rogowski *et al*, 1927; Buss, 1930) and in many other gases, when low over-voltages are applied to uniform-field gaps, whilst the chopped form of voltage decay has been commonly observed (Dehne *et al.*, 1963) to occur at voltages greatly in excess of the static breakdown potential. In a 500 Torr nitrogen spark pulsed in a 2 cm gap, Dehne observed this chopped collapse

for overvoltages greater than 21.5%, whilst for ΔV in the range 16 to 21.5% he observed the stepped form of collapse. For $\Delta V < 16\%$, the gap voltage was observed to initially collapse to the glow voltage and thereafter to decay smoothly to zero. Commenting upon the transition from the stepped to the chopped modes of voltage decay, Dehne maintained that it was brought about by a sudden change in the breakdown mechanism from a regenerative (i.e. Townsend) to a single-avalanche streamer mechanism. Farish and Tedford (1967) and Allen and Phillips (1964) disagree with this conclusion on the grounds that they observed a chopped collapse in humid air, where there have been indications that a regenerative process was operative, and conversely, a stepped collapse was observed for dry air at overvoltages clearly in excess of that required to effect a change in breakdown mechanism. These authors have therefore suggested that caution should be exercised in using only the shape of the voltage collapse profile to deduce the nature of the breakdown process.

Studies have also been made of the dependence of formative times to breakdown (t_f) upon percentage overvoltage (ΔV) applied to the gap, in the hope of gaining further insight into the nature of the breakdown process operative under different discharge conditions. Allen and Phillips (1964) found a discontinuity in the logarithmic plot of t_f against ΔV in their study of breakdown in air, and concluded that this represented the change from the Townsend breakdown mechanism to the streamer mechanism. Later work by Chalmers and Tedford (1975) substantiated the existence of the discontinuity for air, and revealed that in general, a stepped form of voltage collapse occurred when the applied voltage was less than that at the discontinuity (ΔV_d) and that a chopped collapse occurred for overvoltages greater than ΔV_d. Calculations for air and nitrogen have shown that the change in the form of voltage collapse does in fact occur when the number of electrons in the primary avalanche reaches about 10^8. On the other hand, no discontinuity in the logarithmic plot of t_f vs. ΔV has been observed in

the case of nitrogen. Yet there is evidence from calculations, and from image converter streak and shutter photographs (Chalmers, Duffy and Tedford, 1972) that there is a change with increasing ΔV in the nature of the pre-breakdown evolution of discharges in nitrogen, from a slow regenerative type of development to a rapid space-charge accelerated form of growth which occurs in times less than one electron-transit time. Caution should therefore be exercised in using the existence of a discontinuity in t_f vs. ΔV plots to predict whether or not a change in breakdown mechanism has in fact occurred.

On the basis of some of their analytical work regarding formative times in air, together with evidence from the findings of other researchers, Chalmers and Tedford (1975) have cast doubt on the originally proposed mechanism (Raether, 1940) by which streamers are said to propagate from a primary avalanche whose electron number has reached the 'critical' value of 10^8. Raether's model postulates that the only way in which the velocities of the rapidly developing streamers can be accounted for is by assuming that the process of photoionization in the gas occurs at both the front and rear of the critically grown avalanche. Raether discarded the possibility of any cathode secondary process, including photoemission, contributing to streamer development on the grounds that these processes are too slow. Analytical work by Ward (1965) and Davies *et al.* (1971) however, has indicated that the anode- and cathode-directed streamers observed by Wagner (1966, 1967) may be predicted using a model based entirely on a space-charge modified version of the Townsend process, without recourse to gas photoionization. Davies *et al.* showed by a computer-simulation technique that the anode-directed streamer velocities could be adequately accounted for by considering only the effect of the enhanced field in the vicinity of the avalanche head, and furthermore that the rapid cathode-directed front is accurately predictable by considering photoemission from the cathode as the sole secondary electron production mechanism. On the time-scale of less than one electron transit-time, any other secondary emission process would be too slow to contribute. Although the hypothesis of remote ionization of the gas cannot be rejected (Kline,

1974), further recent work by Davies *et al.* (1975), Bayle and Bayle (1974) and Bayle *et al.* (1977) shows the importance of secondary avalanches, due to cathode photoemission, in the very rapid formation of the cathode-directed streamer. Here the streamer develops by the propagation of these secondary avalanches into the high field region at the tail of the critically grown primary avalanche. It appears, on the basis of these findings therefore, that the hitherto used phrase "a change in breakdown mechanism" is imprecise if a cathode process such as photoemission aids, or indeed is a prerequisite for, the accelerated development of an ionized channel. Chalmers and Tedford (1975) concluded that this "change" must in reality be a modification, from a slow to a much faster version of the same fundamental (Townsend-type) mechanism, due to severe space-charge distortion of the applied electric field.

The work of this thesis concerns discharge current growth at very low gas pressures (of the order of 1 Torr) and therefore it is likely that only a slow regenerative type of sparking mechanism is involved here, since the probability of space-charge accelerated development at these pressures is extremely low. For this reason, specific consideration will now be given to spark discharges where this space-charge development is not observed. In particular, an attempt will be made to outline the general features of spark discharges in non-attaching gases at low overvoltages and under both uniform and non-uniform applied-field conditions. Although all of the present work on sulphur hexafluoride sparks was performed under non-uniform field conditions, there is a good deal of information about sparks produced in uniform field gaps that is relevant to this work. This is particularly true with regard to the post-breakdown stages of spark development during which space-charge effects cause non-uniformities in the electric field irrespective of the type of gap used.

A model by which the current growth in a gap at low overvoltage can be represented for a wide range of conditions, is illustrated in Fig. 1.1.(i).

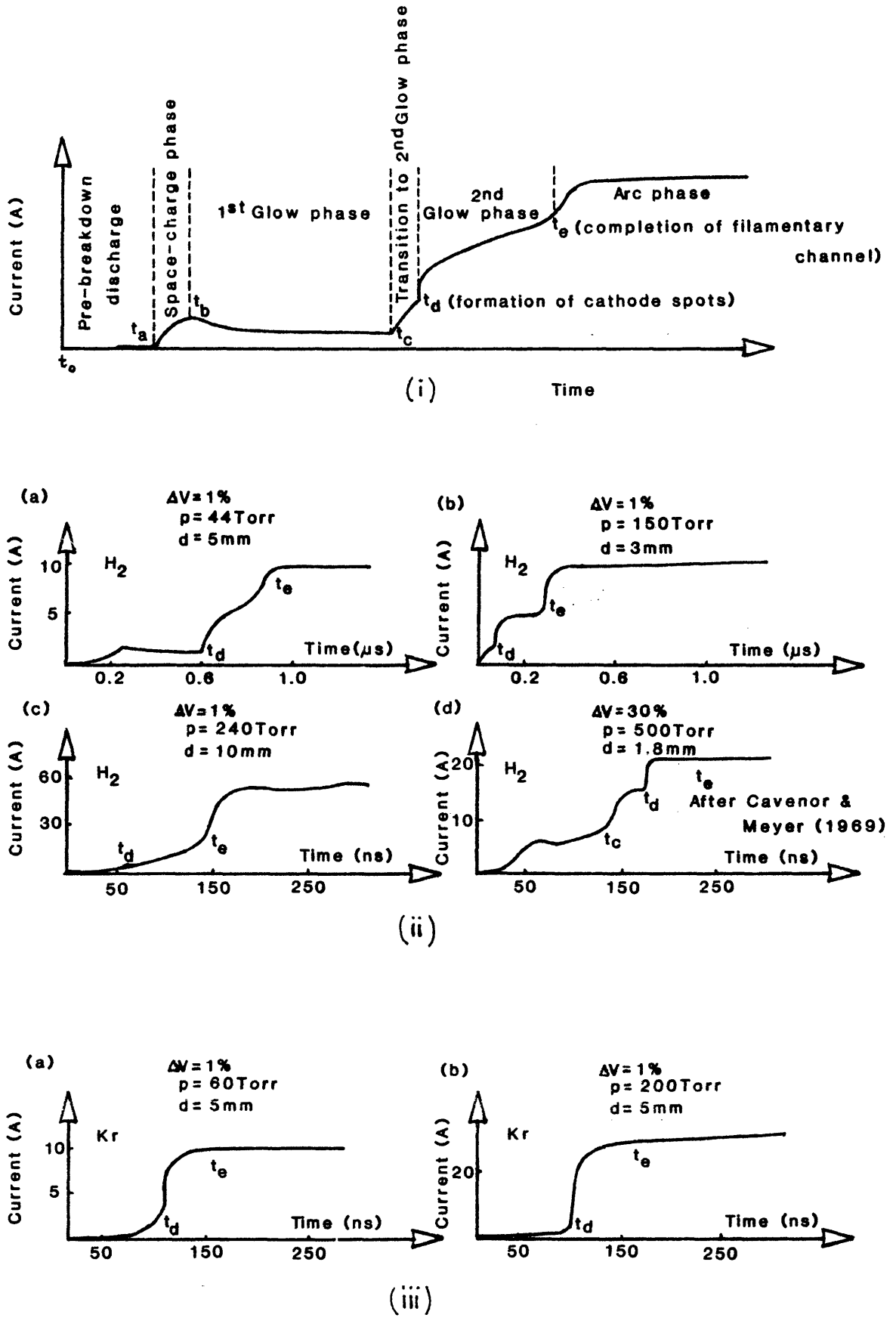

Fig. 1.1 Growth of current curves for two non-attaching gases under different conditions of pressure and gap length;

(i) model of current growth;
(ii) current pulses in hydrogen;
(iii) current pulses in krypton.

This is a slight adaptation of the model originally constructed by Kekez, Barrault and Craggs (1970) who investigated spark channel formation in hydrogen and krypton, by discharging a 50Ω coaxial cable into a small uniform-field gap ($\lesssim$ 1 cm) under conditions of low overvoltage and relatively low pressure (< 250 Torr). The model is intended as a convenient means of defining the different time-intervals used by different workers and it should not be taken as representing an actual current waveform. Figures 1.1.(ii) and 1.1.(iii) show typical current growth curves for low overvoltage sparks in H_2 and Kr for different conditions of pressure and gap length. These have all been obtained by Kekez *et al.* (1970) except for the curve of Fig. 1.1.(ii)d which is due to Cavenor and Meyer (1969), who studied the growth of the H_2 spark under non-uniform field conditions at pressures between 300 Torr and 700 Torr, with electrode separations of a few millimetres and percentage overvoltages of less than 30%. They too utilized a 50Ω coaxial cable discharge system for their investigations.

The first phase of current growth under low overvoltage conditions is the Townsend (prebreakdown) regime and is represented in Fig. 1.1.(i) by the time interval, t_o-t_a. This time is usually called the time-lag to breakdown and is composed of two parts, the statistical time-lag which is the time required for the appearance of a suitably placed initiatory electron, and the formative time-lag, the time taken for the initiatory electron or electrons to generate a sufficient current to bring about a collapse in the applied voltage. In many experimental cases, for applied voltages in excess of the static breakdown potential, V_s, the time-interval, t_o-t_a represents only the formative time to breakdown, as the statistical time-lag is eliminated by the illumination of the cathode by a short burst of ultra-violet radiation, at the instant the voltage pulse is applied to the gap (i.e. at time t_o). The Townsend regime has been investigated in detail both experimentally and theoretically for a number of gases (Rees, 1973) and can be understood in terms of the generation of a succession of electron avalanches

by primary and secondary processes. The currents are in the vicinity of 10^{-7} to 10^{-6} A and a diffuse luminous region develops in front of the anode and gradually expands towards the cathode during this phase.

Following the Townsend regime, is the immediate post-breakdown phase designated by the time-interval, t_a-t_b in Fig. 1.1.(i). It is space-charge dominated, and so is termed the space-charge phase. The currents in this phase can encompass quite a large range from 10^{-6} A to amperes, as for example in some high pressure discharge systems with a low series impedance. The very early parts of this regime have been inaccessible to detailed optical investigation in H_2 due to the relatively low levels of light output, but have been successfully studied in nitrogen (where the light yields are much higher) by Doran (1968, 1969), and theoretically analysed by Kohrmann (1964) and by Davies *et al.* (1975). Doran used a capacitor discharge system in his investigations and subjected a 2 cm uniform-field gap in 300 Torr of nitrogen to an overvoltage of 7.56%. He observed that after the propagation of four Townsend avalanche generations, a series of luminous fronts or "waves of ionization" traversed the gap, resulting in an increase in current to the ampere range. The first luminous front was observed to move towards the cathode and was found to increase in velocity from 5×10^7 cm s^{-1} to 10^8 cm s^{-1} (velocities which are about an order of magnitude greater than the average electron drift velocity). The subsequent fronts were then observed to successively move to and fro across the gap with velocities of around 2×10^8 cm s^{-1}. These fronts have been shown by Doran to be directly associated with the displacement through the gap of local increases in the electric field strength. He suggested that a sudden redistribution of space-charge zones within the discharge, upon the arrival of a luminous front at one electrode, launched a new front towards the other electrode. He observed that this action continued to occur until the gap voltage began to decay significantly. Chalmers *et al.* (1972) observed similar luminous fronts in their studies of

nitrogen in a capacitor discharge system, at both low and high overvoltages. In their low overvoltage investigations, as in Doran's, a quasi-stable diffuse glow phase was seen to form during the propagation of these fronts, with the development of a dark space in front of the cathode. Doran observed that after the discharge current had risen to about 10 A, the gap voltage collapsed from the applied value to that of the glow phase, bringing about the disappearance of the luminous fronts.

Although these ionization waves have not been observed in hydrogen, Köhrmann (1964) has theoretically predicted their existence in capacitor discharge systems in this gas under conditions of high pd (pressure x gap length).

The space-charge phase as observed by Kekez *et al.* and Cavenor and Meyer in their coaxial cable systems also involves (as in the capacitor discharge systems of Doran and Chalmers *et al.*) the development of a diffuse glow structure within the gap. An increase in ionization in the vicinity of the cathode occurs during the early part of the phase through collisions between photosecondary electrons from the cathode and gas molecules. This results in a build-up of positive space charge there and hence in the development of a potential drop across the cathode region. The positive ions gain momentum under the influence of the enhanced cathode field and provide a more prolific emission of secondary electrons in comparison to the earlier photoelectric mechanism. This brings about an increase in ionization and in positive ion accumulation near the cathode, and so further develops the "cathode fall" in potential.

The time t_b marks the completion of the cathode fall development and the establishment of the transient diffuse glow phase. The discharge gap during this regime, t_b-t_c, has been shown by image converter-intensifier shutter and streak photographs to have the same general appearance as the normal d.c. glow discharge, with a negative glow, Faraday dark space and a uniform positive column extending to the anode. Cavenor and Meyer found

the cathode glow and dark space too narrow to distinguish at the high pressures used by them. They measured the potential distribution in the discharge during the first glow phase, t_b-t_c, by the method of Gambling and Edels (1954). Their results gave a uniform positive column field and a cathode fall of 220 V. This value lies within 16% of the corresponding fall for the steady, low pressure normal hydrogen glow discharge for similar electrode material (Cobine, 1941). This agreement with the low pressure d.c. discharge suggested to Cavenor and Meyer that the law of similarity holds even in the transient glow phase, and hence that the product of cathode fall thickness and gas pressure must be a constant. On this basis they calculated the cathode fall thickness to be 1.6×10^{-3} cm for their pressure of 500 Torr, and evaluated the average cathode dark space field to be 1.4×10^{5} V cm^{-1}.

In their particular study of the first (diffuse) glow phase in hydrogen, Cavenor and Meyer found from streak photographs that a partial constriction of the positive column developed during this time. A theoretical model developed by Rogoff (1972) to account for this constriction, will be presented later in this Section.

It has been shown that the size, shape and state of the electrodes have a significant effect on the first glow phase. For example, Kekez *et al.* (1970) have shown that with large plane electrodes, the first glow step is quite prominent, while with point electrodes, it is possible to miss this step entirely. Allen and Phillips (1964) showed that the variation in the duration of the general glow phase for similar conditions of pressure, gap length and electrode configuration, as observed by different workers, was due to the different values of limiting series resistance used. The duration of the first glow phase can be greatly increased by using a large series resistor: clearly this limits the rate at which energy is fed into the gap.

Kekez *et al.* (1970, 1972) found that following the first glow phase in H_2, an intermediate phase, t_c-t_d, could occur (see Fig. 1.1.(i)) depending on the nature of the applied field. If smoothly polished Rogowski profiled

electrodes were used (i.e. providing uniform field conditions) for low overvoltage, low gas pressure (< 240 Torr) and small gap lengths (< 5 mm), this phase was not observed. Instead, t_c coincided with t_d (see Fig. 1.1.(ii) a, b and c) and the discharge proceeded straight into the next phase (the second (filamentary) glow phase). However, for the same general discharge conditions it was observed that if a small enhancement of the initial electric field occurred due to sharp electrode edges or inadequate machining, the intermediate phase, t_c-t_d, would occur perhaps once in a hundred discharges. The phase was regularly detected by Kekez *et al.* for non-uniform field conditions; for example, when using a conical cathode of 160^0 radiused to 5 mm., and a planar anode. It was observed that the phase decreased in duration with increasing gas pressure. Cavenor and Meyer, using a hemispherical cathode and planar anode which were conditioned through repeated sparking, always observed the occurrence of a similar phase (see Fig. 1.1.(ii)d). For clarity, a voltage oscillogram obtained by Kekez *et al.* (1972) has been drawn showing the phases of voltage collapse under the two different applied field conditions (Fig. 1.2). The current profile of Cavenor and Meyer has been converted to a voltage profile and is shown in this figure for comparison. This is legitimate since, as indicated earlier, a strict inter-dependence exists in coaxial cable discharges, between the instantaneous gap current and voltage, so that the profiles of these two parameters are identical.

In their study of this intermediate phase, Cavenor and Meyer found that at time t_c, a luminous filament developed out of the diffuse glow at the anode end and proceeded to propagate towards the cathode. This development continued until the filament reached the positive side of the Faraday dark space. The discharge thus consisted, at this stage, of a distinct cathode fall region (the "cathode dark-space"), diffuse negative glow and Faraday dark space, coexisting with a filamentary positive column. The discharge remained in this mode for about 25 ns until time t_d, when an intense cathode spot was observed to form. From this spot a luminous filament propagated towards the anode at a velocity of about 4×10^6 cm s^{-1}, bringing about a total collapse of the gap

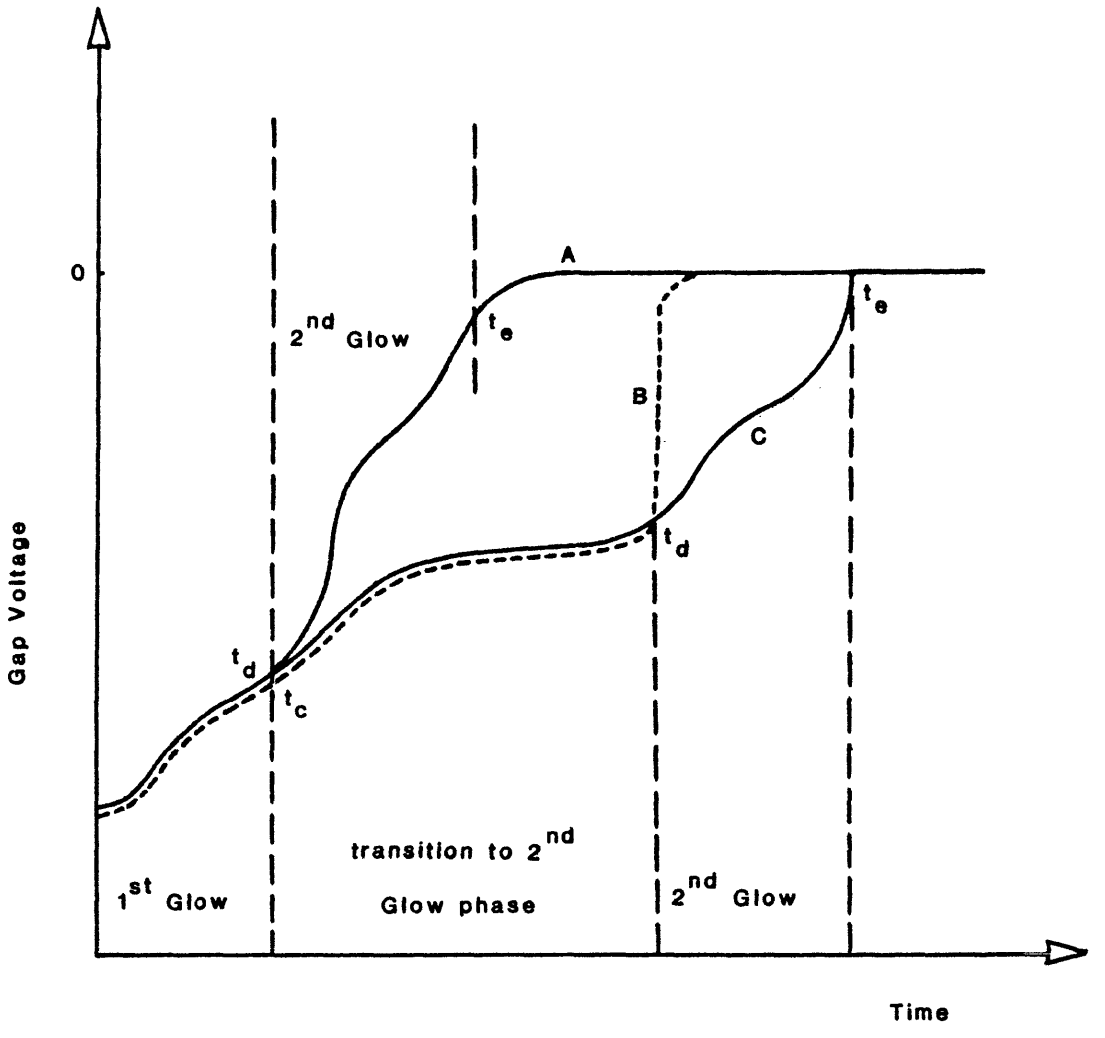

A, Uniform field case (Kekez, et.al.,1972)

B, Non-uniform field case (Cavenor & Meyer,1969)

C, Non-uniform field case (Kekez, et.al.,1972)

Fig. 1.2 A comparison of voltage development in H_2 sparks under uniform and non-uniform applied field conditions.

voltage some 40 ns after time t_d. Spectroscopic investigations by Cavenor and Meyer showed that up to time t_c, the radiation emitted from the positive column was that due mainly to the molecular hydrogen dissociation continuum, whilst after t_c, the radiation consisted predominantly of the line spectrum of atomic hydrogen, suggesting that a substantial increase in dissociation occurred at time t_c. They suggested that thermal dissociation was responsible for the establishment of the filamentary channel. A possible mechanism for this will be discussed later. Kekez *et al.* (1972) mention briefly in the conclusion of their paper, that a contraction of the glow occurs during the intermediate (t_c-t_d) phase, but do not specifically indicate whether the same sequence of events occurs as that observed by Cavenor and Meyer in this phase.

Kekez and co-workers, concerned primarily with discharge development in uniform applied fields, found that under their experimental conditions, an intense cathode spot formed following the contraction and disappearance of the negative zones characterising their first glow phase. The time of this occurrence is shown as t_d in Figures 1.1 and 1.2 and as already mentioned is designated by Kekez *et al.* as the start of the second (filamentary) glow phase, t_d-t_e. The current suddenly rises at time t_d because of the much more efficient cathode-emission mechanism in operation (as compared to the secondary emission due to positive ion bombardment during the first glow phase). The current then attains a quasi-stable level in this phase until such time ($t_d < t < t_e$) when heating of the neutral particles or other processes allow the ionization rate to rise again. As found by Cavenor and Meyer, Kekez *et al.* observed the propagation of a luminous anode-directed filament following the formation of the cathode spot. In hydrogen discharges at low pressure, this has been observed by Kekez *et al.* to be rapidly followed by the propagation of an equally luminous cathode-directed filament from a subsequently developed anode spot. These two oppositely directed

filaments are then observed to link up in the gap bringing about the completion of the filamentary channel, at a time designated by t_e. At this time, or very shortly after, there occurs a complete collapse of the gap voltage to the final arc value. For hydrogen at a pressure of 44 Torr, the intense luminous filaments are observed to propagate towards the centre of the gap with approximately the same velocity of about 1.6×10^6 cm s^{-1}. At higher pressures however, only the anode-directed filament can be observed because of a delay in the development of the anode spot with respect to the formation of the cathode spot.

A qualitative explanation has been advanced by Kekez *et al.* for the propagation of the filaments during the second glow phase. They suggest that the prodigious emission of electrons from the cathode spot causes rapid heating of the neutral gas and ions in the electrode vicinity by energy transfer collisions. Likewise, it is suggested that a similar heating of the neutrals occurs in the region of the anode spot. Consequently, since the neutral gas is hotter near the electrodes than in mid-gap, constriction of a short length of column near each electrode can occur (the role of neutral gas heating in the development of constricted discharges will be discussed shortly). Most of the gap voltage therefore now appears across the non-constricted mid-gap zone and this entails further electron production, and hence neutral gas heating, especially in the zones adjacent to those already constricted. As a result the filamentary zones propagate into the gap until they eventually link up.

It is debatable as to whether the phase t_d-t_e described above should in fact be termed a glow phase, as done so by Kekez *et al.* A new cathode mechanism comes into play at time t_d, which may be field or thermionic emission, but in either case, is more characteristic of an arc-cathode than a glow-cathode. This discharge phase is therefore really a hybrid state, consisting of a combination of an arc-cathode and a glow-column, the latter rapidly developing into an arc-column.

Further investigations into the development of hydrogen sparks in a coaxial discharge system have been carried out by Suleebka *et al.* (1975). These workers used stainless-steel Bruce-profiled electrodes with a separation of 1.6 cm, and used hydrogen pressures ranging between 162 Torr and 460 Torr. They found that with freshly polished electrodes and after 25 shots, the voltage across the gap collapsed in two steps. Out of the diffuse glow phase which initially formed, an anode-directed filament was observed to propagate from a cathode spot. When this filament reached the anode, the gap voltage collapsed to that of the arc phase. This sequence of events was found to be independent of the pressure and overvoltage. When, on the other hand, the electrodes had been well-conditioned, for example after 100 shots, it was found that for a hydrogen pressure of 162 Torr and percentage overvoltages of less than 56%, the gap voltage collapsed in three steps. A cathode-directed filament was initially formed, although there was no evidence of an anode spot associated with it. When this filament reached the cathode, the gap voltage collapsed to its second step value. Then, after a certain time, a cathode spot suddenly developed, bringing about the arc phase. These latter findings obtained for the case of conditioned electrodes, tend to tie in with those of Cavenor and Meyer (who also used conditioned electrodes, as indicated earlier). Further, the observations made when using the freshly polished electrodes support those made by Kekez *et al.* under uniform-field conditions. In addition to these findings, however, Suleebka *et al.* found that when using the conditioned electrodes for a hydrogen pressure of 162 Torr and percentage overvoltage greater than 56%, an anode-directed filament rather than a cathode-directed filament occurred. In this case, there was no evidence of a cathode spot formed before or after filament formation. Suleebka *et al.* also observed that at a critical overvoltage, a filament was generated in mid-gap and propagated towards both electrodes.

It is not presently understood why, when using uniform applied fields and freshly polished electrodes under the conditions of Kekez *et al.* and Suleebka *et al.* a cathode spot and an anode-directed filament always develop first out of the diffuse glow, and are only then followed, if at all, by the propagation of a cathode-directed filament. Furthermore, it is not understood why the reverse sequence of events occurs when conditioned electrodes are used as in the relatively low overvoltage discharges of Cavenor and Meyer, Kekez *et al.* and Suleebka *et al.* Further experimental investigations are required, preferably with the support of theoretical models, in order to explain these repeatedly observed phenomena.

A theoretical model has been proposed by Rogoff (1972) to explain some of the observations made by Cavenor and Meyer of the first (diffuse) glow phase, $t_b - t_c$ in H_2 discharges, preceding the formation of the cathode-directed filament. Rogoff's model describes the role of neutral gas heating in the formation of the partial constriction of the discharge current-density profile, which as indicated earlier, was observed to progressively occur during the diffuse glow phase.

Employing the discharge parameters of the Cavenor and Meyer experiment, Rogoff calculated for the positive column, the temporal evolution of the spatial distributions of the gas number density, radial gas velocity, gas temperature and current density, i.e. $N(r,t)$, $v_r(r,t)$, $T(r,t)$ and $j(r,t)$ respectively. The first three of these quantities were evaluated from a numerical analysis of the conservation equations of mass, momentum and energy, in conjunction with the equation of state for a perfect gas. For the current density, $j(r,t)$, Rogoff derived a semi-empirical expression in terms of the gas number density $N(r,t)$ and the longitudinal electric field E (this field was assumed independent of time and position in the column for the diffuse glow period). Neglecting the effects of the radial transport of charged particles, Rogoff assumed the current density to be given by the equation:

$$j(r,t) = n_e(r,t)\, e\, v_d(r,t) \qquad (1.1b)$$

where n_e and v_d are the electron number density and drift velocity respectively, and e is the electronic charge. An empirical evaluation was made of the dependence of n_e and v_d on the gas number density N and electric field E for the conditions of the Cavenor and Meyer experiment. The resulting expression obtained for the current density was

$$j(r,t) = A\, g(r)\, E^{3/2}\, N^{-1/2}\, (r,t).\exp\left[\frac{-BN(r,t)}{E}\right] \qquad (1.1c).$$

Here A and B are constants and the function g(r) is a quantity which describes the radial distribution of the electron number density at the beginning of the diffuse glow phase (i.e. at $t = t_b$). Rogoff showed that the electron drift velocity v_d is independent of radius at time t_b, so that $j(r,t_b)$ as well as $n_e(r,t_b)$ is described by the function g(r). Rogoff took g(r) to be approximated by the radial light intensity profile of the H_2 dissociation continuum measured by Cavenor and Meyer just after the formation of the diffuse glow at 400 Torr. This approximation was justified on the basis that the observed radiation was essentially due to electron-molecule collisions, and that the neutral number density was independent of radius at time t_b.

From a knowledge of the parameters A, B, g(r) and E, Rogoff numerically solved equation 1.1c, to obtain the radial current-density distribution as a function of time, by using the appropriate gas density profile in each case. The numerical solution of the conservation equations mentioned earlier provided these values of N(r,t). The analysis of N(r,t) showed that radial expansion of the heated gas occurs during the diffuse glow phase, t_b-t_c, and that by time t_c, the gas number density has decreased by as much as 10% on the axis, whilst it has increased off axis. Equation 1.1c shows that the gas density strongly controls the current density, with a decrease in N bringing about a rapid increase in j. Rogoff thus showed that an accelerated development in current density occurs in the axial regions during the diffuse glow phase and that there is a simultaneous drop in j in the outer zones. Rogoff attributed the development of the partial constriction of the current channel observed by Cavenor and Meyer to this change in current density profile.

Rogoff's calculations were performed for times up to and well beyond time t_c (i.e. the end of the diffuse glow phase). However, no abrupt charges in discharge properties such as those observed experimentally by Cavenor and Meyer to occur at time t_c, were indicated. The profiles of temperature, gas density and current density appeared as smooth extensions of the development prior to t_c. Thus the theory predicts a smooth transition from a diffuse to a constricted mode of discharge. Rogoff attributed this prediction to the exclusion of dissociation effects in the calculations. As indicated earlier, Cavenor and Meyer (1969) showed spectroscopically that gas dissocation effects in hydrogen become significant at time t_c. Although the theory of Rogoff is inadequate in explaining the sudden current transition in hydrogen at time t_c, it is consistent with experimental observations of discharge growth in monatomic gases, such as in krypton as studied by Kekez *et al.* (1970), where dissociation effects are absent. In this case, a smooth transition is observed to occur from the diffuse to constricted phase (see, for example Fig. 1.1.(iii)a).

From the computed radial temperature profiles, Rogoff deduced the axial temperature at time t_c to be approximately 2250 K, which is the value at which dissociation effects in hydrogen should start to become significant. The same temperature profiles also indicated that from time t_c onwards, the axial gas-temperature increases smoothly, but more rapidly than before. This suggests that there should be an accelerated production of atomic hydrogen on the discharge axis after time t_c. On this basis, Rogoff concluded that processes like rapid dissociation must play a major role in the sudden development of the filamentary core in the hydrogen discharge column.

It is not yet fully understood how the process of dissociation is connected with the discharge contraction. However, Rogoff suggested that the sudden production of atomic hydrogen will remove molecular (especially vibrational) excitation as an electron energy-loss mechanism, and so would result in a more pronounced high-energy tail in the electron energy distribution. This would lead to an increase in the rate of ionization. Since atomic hydrogen has an ionization

potential 12% lower than that of molecular hydrogen, the ionization rate would be even further enhanced. This would rapidly promote thermal dissociation due to neutral gas heating, while the latter process would sharply accentuate the existing gas density profile to give a constricted current density distribution. Rogoff suggested that this would occur simultaneously everywhere in the positive column if the field is uniform, but that the filamentary core formation might be expected to occur first in any local region where the field is higher. As discussed earlier, Cavenor and Meyer observed the formation of a luminous filament (at time t_c) at the anode end, which then propagated towards the cathode region. Rogoff explained the formation of the filament at the anode end on the basis of the field there being higher than in the main column.

Relatively simple calculations have been performed by other workers, such as Chalmers *et al.* (1972) on the velocity of luminous filaments in discharges assuming that their propagation is brought about by molecular dissociation. Studying the development of a nitrogen spark at 300 Torr and $\Delta V = 5\%$ in a 3 cm uniform-field gap, Chalmers *et al.* experimentally observed filaments propagating from the electrode regions and meeting in mid-gap to bring about the glow-arc transition. The measured and calculated values of the filament velocities were in good agreement (6×10^6 cm^{-1} and 8×10^6 cms^{-1} respectively), thus substantiating the suggestion that filament propagation is brought about by thermal dissociation.

Another model which has been proposed for the rapid propagation of the luminous filamentary channel is one due to Kekez and Savic (1974) based on detonation-wave theory. They postulated that once the filamentary-channel has been initiated in a glow discharge, a local "explosion" occurs at the tip of the channel by the sudden transfer of energy to the ions and neutrals from electrons heated by electric-field concentration in front of the tip. Since this field concentration is strongest at the axis of the channel the electrons there will be preferentially heated, and hence the spark channel will tend to elongate mainly in the direction of the channel axis. The sudden thermalization

of the heavy particles at every instant, producing the continual extension of the channel tip, also drives a shock-wave in all directions. This shock-wave has its maximum strength in the direction of the channel axis and it has been shown that for hypersonic elongation of the spark channel, the advancing shock-front which surrounds the channel tip is of paraboloidal shape. The mechanism described here for the channel- and shock-wave-propagation is analogous to that which drives detonations through explosive gas-mixtures. In these detonations, a combustion zone closely follows an advancing shock-front and the chemical energy released by the gases in combustion provides the power for the continued propagation of the shock-wave (Gaydon and Hurle, 1963). On the basis of this analogy therefore, Kekez and Savic have employed the so-called Chapman-Jouguet condition for detonations, in conjunction with appropriate field-theory, to derive the velocity of the discharge shock-front, and hence that of the spark channel head, in terms of the length of the developing channel. Kekez and Savic found experimentally that the motion of channel development in a 162 Torr hydrogen spark pulsed in a 1.9 cm uniform field gap at an overvoltage of 0.01%, proceeded with constant velocity in the first 10 to 20% of the total gap length measured from the cathode (the use of uniform applied fields and freshly polished electrodes gave rise to the formation of cathode spots and anode-directed filaments before the formation of cathode-directed filaments). From about 25% up to about 50% of the gap length, the velocity of the anode-directed filament was found to increase rapidly. Use of the detonation wave model yielded velocities in good agreement with experiment for a number of gases (such as the rare gases and hydrogen) at low pressure, low overvoltage and up to certain positions within the gap. This agreement was found to be unsatisfactory however, at high pressures, for example in the case of hydrogen at 400 Torr where the measured velocity was about eleven times that calculated. Work by Suleebka *et al.* (1975) showed that the measured channel velocities under the same conditions as those employed by Kekez and Savic at high pressure, were even higher than those quoted by the latter pair of workers.

To account for some of these differences, Kekez and Savic (1975, 1976) developed variations of their original (1974) hypersonic model of spark channel propagation. By using their so-called "hypersonic-hyperboloidal" model, much better agreement was obtained with the results of Suleebka *et al.*'s experiments. Kekez and Savic therefore suggested that their original hypersonic model only described propagation at the very earliest stages of motion in the case of high pressure discharges.

Yet another shock-wave model has been proposed by Kekez and Savic to account for filament velocities at larger distances from the point of propagation within a gap (for which conditions, the hypersonic models are inadequate). They proposed the "cold" and "hot" Volterra models, the basic mechanisms of which involve the local field at the channel tip not only causing electron heating of the gas molecules (as in the case of the hypersonic models) but also electron multiplication at the tip. Comparison of experiment and theory using these "Volterra" models, gives order of magnitude agreement.

1.2 SPARK DEVELOPMENT IN ELECTRONEGATIVE GASES

Numerous studies regarding breakdown and discharges in electron-attaching gases have been made by different workers in past years. The early studies of electronegative discharges mainly involved low pressure and low current d.c. glows. Such discharges have been studied, for example, in iodine vapour (which is strongly electronegative) by Spencer-Smith (1935a,b) and Emeleus and Sayers (1938). Studies relating to the time-lag to breakdown, and to the breakdown process itself, have been carried out in various electronegative gases including oxygen, sulphur hexafluoride and some halogen derivatives of methane, such as "Freon" (Meek and Craggs, 1978). With regard to SF_6 discharges, a considerable amount of research has centred on the electrical and thermal properties of high pressure SF_6 arcs (Frost and Liebermann, 1971; Lowke and Liebermann, 1971; Hertz *et al.*, 1971). Interest in both the breakdown and arc properties of SF_6 have arisen from the practical importance of this gas in the electricity supply industry (see Section 1.3.4).

In contrast to the amount of published work on the topics mentioned above, comparatively little information is available regarding the growth of spark discharges in electronegative gases. Research in the latter area has been limited to oxygen, iodine and SF_6. A discussion will now be presented on the development of spark discharges in these gases, as studied by various workers.

1.2.1 Oxygen

Although an abundance of information exists on the electronic, ionic and atomic collision processes which occur in oxygen, only two significant papers on spark discharges in this gas have appeared in the literature within the last two decades. The first of these, by Allen and Phillips (1964) deals mainly with the variation of formative time-lag with overvoltage and pressure for a number of gases including oxygen, whilst the second paper

by Chalmers, Duffy and Tedford (1972) concerns the later stages of development of sparks in different gases including oxygen and SF_6.

Allen and Phillips obtained time lag data for the development of currents in oxygen by observing the voltage waveform of an oxygen spark produced between uniform-field brass electrodes. The cathode was irradiated with a burst of ultraviolet radiation immediately following voltage application, and the formative-time taken as the time that then elapsed before gap-voltage-collapse occurred. It was found that for pd values ranging from 750 Torr cm to 2250 Torr cm, a log-log plot of formative time (t_f) against percentage overvoltage (ΔV) exhibited a pronounced discontinuity in the 1 to 2% overvoltage region. As with their interpretation of a similar discontinuity in the t_f vs. ΔV plot for air (see Section 1.1) Allen and Phillips suggest that a transition occurs in the form of development of the oxygen spark at these low ΔV, from a regenerative- (Townsend-) to a space-charge accelerated- (streamer-) mechanism. Allen and Phillips showed from "still" photographs of a 250 Torr O_2 spark pulsed in a 3 cm gap at an overvoltage of 8%, that a luminous filament extends from cathode to anode, with a bright "knob" located at some fixed distance from the anode. The position of this bright knob was identified with the position in the gap at which streamer formation was thought to have taken place. A calculated value of this position, based on the Meek criterion for streamer breakdown (Meek, 1940), was found to be in good agreement with the experimentally observed value. This agreement was found to hold over a wide range of overvoltages.

A more detailed investigation of the properties of oxygen sparks was carried out by Chalmers *et al.* (1972) who used an image converter and a 4-stage image intensifier, as well as oscillographic techniques, to study the growth of sparks in a 3 cm, uniform-field gap for overvoltages up to 25% and pressures from 100 Torr to 300 Torr. They found that under their experimental conditions, the development of oxygen sparks at high overvoltages ($\sim$ 25%) was similar to those at low overvoltages ($\sim$ 1%). In both cases, a

bright luminous region was observed to develop at a point within the gap. At lower overvoltages, this was found to occur several hundreds of nanoseconds after voltage application. From the luminous region, intense filaments were observed to propagate towards the two electrodes at high speeds ($\sim 10^7$ cm s^{-1}) bringing about the arc phase shortly after bridging the gap. The voltage waveforms obtained showed no signs, at any overvoltage, of being step-like in appearance, indicating that no transient glow phase occurred (this is supported by the results of the streak and shutter photographs). Calculations similar to those performed by Allen and Phillips with regard to the position of the bright luminous region from which the filaments propagate, suggested that, for both the high and low overvoltage cases, this position corresponds to that at which the primary avalanche achieves an electron population of 10^8. The streak records however, showed no evidence of anode- and cathode-directed streamers (see Section 1.1) which should theoretically have completely bridged the gap within the transit-time of the primary avalanche (it should be noted that these streamers are not to be confused with the intense filaments which lead to the arc channel). Nevertheless the shutter records, for the high (25%) overvoltage case, indicate a narrow filament which appears to have reached the anode in times less than one electron-transit-time. Chalmers *et al.* suggest that this anode-directed propagation may have been an anode-directed streamer. No simultaneous cathode-directed luminosity was observed however. This anomaly, together with the long delay observed at low overvoltages, between the onset of luminosity in the gap and the final constriction of the discharge have been explained on the assumption that photons emitted from the head of the primary avalanche were delayed in their journey towards the cathode due to some type of resonance process.

1.2.2 Iodine

Electrical discharges in iodine vapour have been studied for about the last fifty years, although mainly under d.c. conditions. Emeleus and Woolsey (1970) have compiled a number of papers dating back to 1935, which describe the fundamental physical properties of d.c. iodine discharges as studied by various workers. The only detailed investigations of spark discharges in iodine vapour, however, have been carried out by Lewis and Woolsey (1971 and 1981). In the more recent of their two papers, Lewis and Woolsey give a detailed description of the various phases and transitions which have been observed to occur in low-pressure iodine sparks (0.08 Torr to 0.80 Torr) pulsed in a 10 cm, non-uniform field gap at between 1 kV and 3 kV, corresponding to overvoltages of up to 300%. Image converter and oscillographic techniques were used to investigate the various phases of spark growth and decay. These phases are represented with their relevant time-intervals in the schematic diagram of Fig. 1.2.2.(i) which shows current growth as a function of time for an iodine spark of pressure 0.36 Torr, gap length 10 cm and overvoltage 265%.

The first phase, called the post-breakdown phase ($t_A < t < t_B$) was inaccessible to detailed study due to electrical noise problems. However, the current and voltage oscillograms obtained, suggest that a very rapid rise and fall in ionization growth occurs during this phase which lasts for about 500 ns.

During the glow phase ($t_B < t < t_D$), relatively small currents, averaging about 30 mA, were observed to flow through the discharge. The light output during this phase was not intense enough to allow useful time-resolved photographs to be obtained. Information about the phase was obtained however, from measurements of axial potential distribution. The general technique that was used to do this is similar to that of Cavenor and Meyer (1969). The method will be outlined later when discussing potential distribution measurements in the low pressure SF_6 spark. Lewis and Woolsey measured high cathode-fall voltages averaging about 2450 volts during the glow phase,

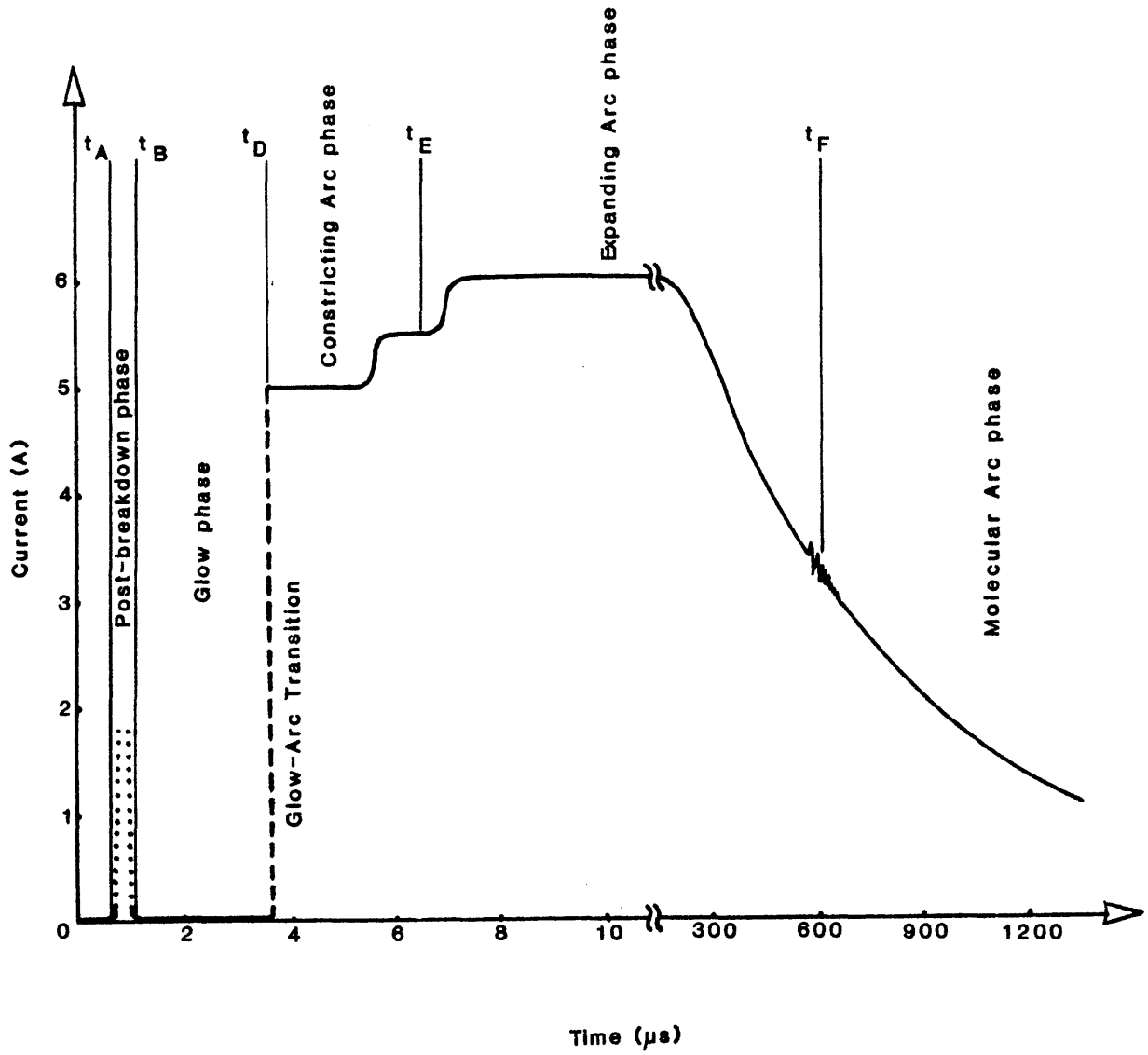

Fig. 1.2.2.(i) Profile of current growth in a 0.36 Torr, 10 cm iodine spark pulsed at an overvoltage of 265% (as observed by Lewis and Woolsey, 1981).

and a positive column field which remained constant throughout the phase, at 44 ± 4 Vcm^{-1}. They suggest that the high cathode falls, which were similar to those obtained in d.c. iodine discharges at similar currents, indicate that this quasi-stable phase is an abnormal glow. They further suggest that the combination of low discharge current, high cathode fall and relatively high column field indicate that attachment plays an important role throughout the glow phase.

At time t_D, an abrupt increase in current to about 5A was observed to occur, while the gap voltage fell to around 500 volts, both within 20 ns of t_D. This transition was accompanied by the production of a bright cathode spot, which was always found to occur at the boundary between the metal cathode and an adjacent insulator. It was observed that if no such boundary existed, the transition was inhibited. The appearance of the cathode spot, together with the rapid rise in current, and fall in voltage at time t_D, has been taken to indicate a cathodic glow-arc transition characterised by an abrupt change in the process of secondary electron emission from the cathode. The authors point out that the energy delivered to the cathode during the glow phase was too small to induce thermionic emission, and that field emission was the most likely process to take over from the glow mechanism of secondary electron emission due to positive ion bombardment. The authors also advance an explanation as to why the cathodic glow-arc transition in iodine takes place at currents in the milliampere region, in contrast to transitions in non-attaching gases which are usually generated from much larger amplitude glow currents. They suggest that in the transient iodine glow, the positive and negative ion number densities are much greater than the electron number density, in view of findings by Plumb *et al.* (1973). Plumb *et al.* made Langmuir probe measurements in a d.c. iodine discharge at a pressure similar to the iodine spark studied by Lewis and Woolsey, and obtained a negative-ion-to-electron number density ratio of the order of 10^3. Lewis and Woolsey suggest that if such a high ratio exists in the transient glow, then even though the electron current, and hence discharge

current, are low, a high positive-ion flux can still exist at the cathode, just as would be found in much higher current glow discharges through non-attaching gases. Lewis and Woolsey point out that this could account for the glow-arc transition at such low glow discharge currents, since the field-emission mechanism depends on positive ion bombardment of the cathode rather than on the total discharge current.

The phase following the glow-arc transition is defined by Lewis and Woolsey as the constricting arc phase which spans the time-interval $t_D < t < t_E$ (see Fig. 1.2.2.(i)). For this phase, a series of time-resolved image converter pictures was taken. These show that constriction of the diffuse positive column occurs in two stages. Following the formation of the cathode spot at t_D, constriction begins at the cathode-end of the column and progresses towards the anode at a rate of about 2×10^6 cm s^{-1}, while the discharge current and voltage remain constant at 4.5A and 560 volts, respectively. About 2 μs after time t_D, the anode-end of the positive column is observed to constrict as a whole rather than progressively from the cathode-end. Simultaneous with this second stage of constriction, the discharge current increases and the gap voltage falls, until at time t_E, the entire positive column has become constricted. Axial potential distribution measurements for times during the constricting phase show that the column fields in the unconstricted zones remain constant at about 50 ± 5 Vcm^{-1} although a high field of about 100 Vcm^{-1} exists, which can be identified with the position of the anode head of the propagating filament. The cathode fall collapses from a value of about 90 volts at times beyond t_D. Lewis and Woolsey suggest that the discharge constriction and filament propagation are due to thermal dissociation, as earlier suggested by Cavenor and Meyer (1969), Rogoff (1972) and Chalmers *et al.* (1972). They performed a calculation based on one done by Chalmers *et al.* to obtain the velocity of the anode-directed filament on the basis that all the energy delivered to the gap goes into thermally dissociating the gas. They obtained a value an order of magnitude larger than their measured velocity and suggest

that the discrepancy could be accounted for by (a) other energy transfer processes in the column, in addition to molecular dissociation and (b) by the likelihood that the head of the propagating filament has a larger cross-section than that of the established arc column (the propagation velocity of the filament is inversely proportional to its cross-sectional area, and in the calculations, the established arc cross-section was used). The authors also explain that the sudden constriction of the anode region which occurs independently of the propagating filament, some 2 μs after t_D, suggests that the energy supplied by the circuit must have been sufficient in that 2 μs period to raise the temperature in the anode region above that required to initiate dissociation. This hypothesis was essentially verified by the result of a calculation relating the energy supplied per unit length of positive column in time t, to that absorbed by unit length of column. The authors propose that the actual mechanism by which dissociation gives rise to constriction in iodine, may be associated with the electronegative nature of the gas. They suggest that when dissociation becomes important at around 1000 K, the attachment rate will fall, since in iodine, attachment is primarily a dissociation process involving I_2 molecules (Biondi and Fox, 1958). They state that this would provide an increase in electron density in the dissociation region and a corresponding rise in electrical conductivity. In turn, this would produce further gas heating and dissociation, as well as increased ionization, culminating in a filamentary discharge.

About 1 to 2 μs after the completion of the positive column constriction at time t_E, the electrical conductivity is observed to increase, with a substantial drop in the column field from about 50 Vcm^{-1} during the constricting phase to about 6 Vcm^{-1}. Within a few μs after t_E, the arc column is seen, from the time-resolved pictures, to suddenly expand in cross-section. It is suggested that this is due to a rapid pressure increase which develops in the constricting arc phase. Continued expansion then occurs at a slower rate, due to radial thermal diffusion. The authors calculate that

at a time 20 μs after t_D (at which time the column field is only 2 Vcm^{-1}), the arc temperature would have reached 5000 K and that the electron number density in the column would be 6 x 10^{12} cm^{-3}.

The final transition observed in the low pressure iodine spark occurs at time t_F, some 600 μs after time t_D. At this stage the positive column field is observed to suddenly increase from 2 Vcm^{-1} to 18 Vcm^{-1} with the cathode fall remaining at 20 volts. Together with this, the discharge current, which by time t_F has fallen to about 3A due to dissipation of charge from the external storage capacitor, decreases in its rate of decay. Lewis and Woolsey attribute the transition to a rapid change from an atomic to molecular arc phase. They explain that the arc temperature would naturally fall, as the positive column expands, and the discharge current falls after time t_E. When the arc temperature decreases below 1000 K, substantial re-association would occur. This would bring about an increase in the thermal conductivity of the gas and hence in an acceleration of the cooling process, and would thus induce a rapid transition from an atomic to molecular arc column.

1.2.3 Previous Studies of Spark Development in SF_6

Sulphur hexafluoride is a technically important electronegative gas which is widely used in the electricity supply industry and in other applications. Its importance has promoted fundamental research into the molecular collision processes occurring in the gas, and also into the properties of SF_6 arcs (some of these properties and applications will be presented in Section 1.3). As with oxygen, however, relatively little time-resolved work has been done on spark development in this gas. The only significant work on SF_6 has been done by Chalmers *et al.* (1972). Pfeiffer and Schmitz (1978) added a little to the existing knowledge by photographically investigating channel development in compressed SF_6. Most of the other research, to date, on SF_6 sparks however, has been concerned with time lag measurements.

Craggs and Meek (1962) measured formative times in SF_6 for a variety of electrode configurations, using a capsule of Cobalt 60 to irradiate gaps up to 3 cm in length. For uniform-field gaps subjected to small overvoltages ($\lesssim$ 1%) long time lags of several hundreds of microseconds were observed. However, for overvoltages of 2%, the formative times decreased to only several microseconds. Due to the flow of a steady primary current of 10^{-12} A, Craggs and Meek suggest that the long time lags observed are probably not caused by a delay in the appearance of an electron that could initiate breakdown, but are associated with the mechanism of spark-breakdown. For a negative point-plane gap in SF_6 at 200 Torr, the authors showed that at overvoltages of about 1%, the formative times exceeded a millisecond, whilst overvoltages of up to 30% were required to reduce the formative-time to 1 μs. For positive point-plane gaps of similar separation, they found that an overvoltage of 15% was required to reduce the formative time to 1 μs.

More extensive studies were made by Kuffel and Radwan (1966) on the effect of such factors as cathode irradiation, gap length, gas pressure and electrode conditioning, on time lags in SF_6. At low overvoltages and for conditions of cathode illumination, time lags were found to be long and highly scattered compared with those in air obtained under similar conditions. For a uniform-field gap of length 1.5 cm, pressure 100 Torr and overvoltage 10%, the time lags were found to vary between about 1 and 43 μs. The average time lags and scatter decreased with increasing overvoltage and with increasing gap length. As expected the average time lags and scatter increased in the absence of irradiation. Kuffel and Radwan also observed that when the over-voltage was plotted as a function of the average time lag, a distinct time lag-free region was obtained between two separate groups of average time lag. It was suggested that this time lag-free region results from a change, with overvoltage, in the negative-ion species formed by attachment of electrons to the neutral gas molecules and radicals.

Chalmers *et al.* (1972) confirmed the existence of a time lag-free region in SF_6 and obtained time resolved photographs of SF_6 sparks for overvoltages corresponding to time lags on either side of the time lag-free region. They showed that some distinct differences exist between the types of development obtained under the conditions corresponding to the two groups of time lags. For a pd value of 300 Torr cm and for low overvoltages ($\sim$ 3%) corresponding to the group of longer time lags, their image converter shutter photographs show a faint luminous track extending across the gap 500 ns after voltage application. This luminous track is seen to increase in intensity and to radially expand in time for about 800 ns, following which a constricted region of luminosity evolves at the anode and rapidly propagates towards the cathode, expanding radially as it develops and producing a cone-shaped discharge. Shortly after the initiation of this cathode-directed propagation, a similar type of discharge is observed to propagate from the cathode. However instead of proceeding to meet in the gap (as is observed to occur with the luminous filaments originating at the electrodes in hydrogen and nitrogen at low overvoltage), these conical discharges cease to propagate after each has extended a distance of one-third the gap length from the electrodes. This leaves a broad dark space between these discharges. At this stage the gap voltage is observed to start significantly collapsing. The central dark space persists for a few tens of nanoseconds before it brightens to form a diffuse discharge which remains separated from the conical discharges by relatively thin, but well-defined dark spaces. Very shortly ($\sim$ 50 ns) after the formation of the diffuse discharge in the central dark space, a filamentary discharge develops across the gap, bringing about the complete collapse of the gap voltage to the arc value. As was found in high pressure oxygen sparks at very low overvoltages, no transient glow phase occurs in the development of this SF_6 spark.

At higher overvoltages ($\sim$ 8%) corresponding to the groups of shorter time lags, the development of ionization is far more rapid than at 3%. A thin luminous track is found to extend across the gap only 90 ns after voltage

application. This is comparable with the faint track observed to occur soon after voltage application in oxygen at an overvoltage of 25%. However, whereas in oxygen, the thermal dissociation phase (i.e. that corresponding to the propagation of the intense luminous filaments) was subsequently initiated somewhere in the gap, in SF_6 an intense filament is initiated at the cathode some 150 ns after the formation of the luminous track, and propagates towards the anode at a velocity of about 10^7 cm s^{-1}. At the same time, the gap voltage begins its collapse to the arc value. Considerable radial expansion of the filament is observed to occur by the time it has reached mid-gap. Shortly after the initiation of this filament, a similar but less intense one is observed to propagate into the gap from the anode, rapidly expanding radially, as it progresses. A well-defined dark space is then observed to separate the resulting broadened zones of luminosity in mid-gap. The rate of collapse of the gap voltage then increases, until some 50 ns after the formation of the central dark space, a highly conducting arc channel becomes established.

On the basis of calculations using the original streamer criterion (Meek, 1940), the phenomena observed by Chalmers and co-workers have led them to conclude that for their experimental conditions, the breakdown of SF_6 even at voltages only slightly in excess of the static breakdown voltage, is preceded by space-charge-accelerated development of the primary avalanche. No definite conclusions are reached however, regarding the nature of the complex processes observed to occur after the primary avalanche has attained its critical electron population (of $\sim 10^8$).

Pfeiffer and Schmitz (1978) investigated development up to spark channel formation in compressed SF_6 at zero overvoltage using oscillographic, photographic and photomultiplier techniques. A coaxial-cable discharge system was used in this work (in contrast to the capacitor discharge system used by Chalmers *et al.*) to facilitate the high degree of temporal resolution required

(∿ 1 ns). The distributed capacitance of the special coaxial-cable was slowly charged until the voltage built up was just sufficient to break down a hemispherical electrode gap which formed a break in the central conductor of the cable. The prebreakdown regime was observed to last less than 10 ns for a gas pressure of 900 Torr and a gap length of between 5 and 7 mm. Using a photomultiplier tube, two types of prebreakdown luminosity development were observed to occur. The authors suggest that one type might be due to the Townsend mechanism and the other to the streamer mechanism of discharge growth. They have not been able however, to confirm this hypothesis. The corresponding image intensifier results do not show a marked difference. In both cases, a cathode-directed filament originating near the anode, develops out of a diffuse glow. A few differences however, are evident in the rate of development within the first 4 ns of breakdown-voltage application. The image intensifier results obtained for the supposed streamer breakdown case, bear no resemblance to those obtained by Chalmers *et al.* at low overvoltage (3%).

In summary, it may be concluded that although the gross properties of sparks in SF_6 are known for a few specific experimental conditions, the precise mechanisms of spark evolution in this gas at high pressure (as in high pressure oxygen) are still far from being understood. Further experimental and computational studies are needed to clarify these growth mechanisms, and in particular the role played by the processes of electron attachment and detachment.

1.3 PROPERTIES AND APPLICATIONS OF SF_6

1.3.1 Introduction: Basic Properties

Sulphur Hexafluoride (SF_6), which is a gas at S.T.P., is commercially produced by burning sulphur in an atmosphere of fluorine, and removing the lower fluorides such as S_2F_2, SF_4 and S_2F_{10}, by pyrolysis. The gas is colourless, odourless, tasteless, non-toxic and non-flammable under ordinary conditions (Schmidt and Siebert, 1973). The sulphur atom of the SF_6 molecule possesses six equivalent sp^3d^2 hybrid orbitals, with each orbital accommodating one valence electron from one fluorine atom, together with one from the sulphur atom. This particular bonding gives the molecule a regular octahedral structure, with the sulphur atom located centrally and each fluorine atom at one of the six corners. This highly symmetric structure renders SF_6 chemically inert. A list of fundamental physical properties of SF_6 is presented in an article by Schumb (1947), whilst a comprehensive list of thermochemical data such as the heat capacity at constant pressure, entropy, the "free energy" function, enthalpy, etc. is available as a function of temperature (from 0 to 6000 K) in the JANAF Thermochemical Databook (1965).

One of the most important properties of SF_6 is that it is strongly electronegative, i.e. it has the ability to form stable negative ions by the attachment of electrons to the neutral molecules. Together with its chemical inertness and electronegativity, the electrical and thermal transport properties of SF_6 arc plasmas, make this gas highly suitable for use in certain important technical applications in the electricity supply industry. The extent of its use, however is limited in part to its relatively low liquefaction pressure of 22.5 atmospheres at 298 K.

The transport properties of the SF_6 arc will be discussed in the following Section 1.3.2, and after a description in Section 1.3.3 of

the fundamental electronic processes in Townsend and established glow discharges in SF_6, consideration will be given in Section 1.3.4 to some applications of SF_6 discharges.

1.3.2 The Properties and Behaviour of SF_6 Arc Plasmas

In general, the behaviour of arc plasmas in local thermodynamic equilibrium (LTE) can be described by thermodynamic laws and macroscopic quantities such as the electrical and thermal transport properties, without requiring any specific knowledge of the individual collision processes that occur in the plasma (Maecker, 1964a). This is because in these thermal plasmas, where the electron and gas temperatures are comparable, energy is transferred to the neutral gas predominantly through elastic collisions with electrons.

In order to calculate the transport properties of SF_6 and their variation with arc temperature, it is necessary to know the particle composition in the SF_6 plasma and the variation of particle density with arc temperature. By considering a total of 24 molecular, atomic and ionized species, Frost and Liebermann (1971) have calculated, assuming LTE, the composition of the SF_6 plasma, by means of a thermodynamic method involving the minimization of the Gibbs free-energy. Their calculations have been performed for pressures of 1, 2, 4, 8 and 16 atmospheres, over a temperature range extending up to 45000 K. The results obtained for the composition of the SF_6 plasma at 1 atmosphere are in general agreement with the earlier calculations of Frie (1967) whose (less extensive) results are reproduced in Fig. 1.3.2.(i). It can be seen from this plot that at around 2100 K, the SF_6 molecule dissociates rapidly with large simultaneous increases in the concentrations of free fluorine and sulphur atoms. The concentration of ionized sulphur S^+ at the lower temperatures is found to be considerably higher than that of F^+ due to the lower ionization potential of sulphur (10.4 eV) in comparison to fluorine (17.4 eV). It is only when the temperature exceeds $\sim$ 13000 K, that the F^+ concentration starts to exceed that of S^+.

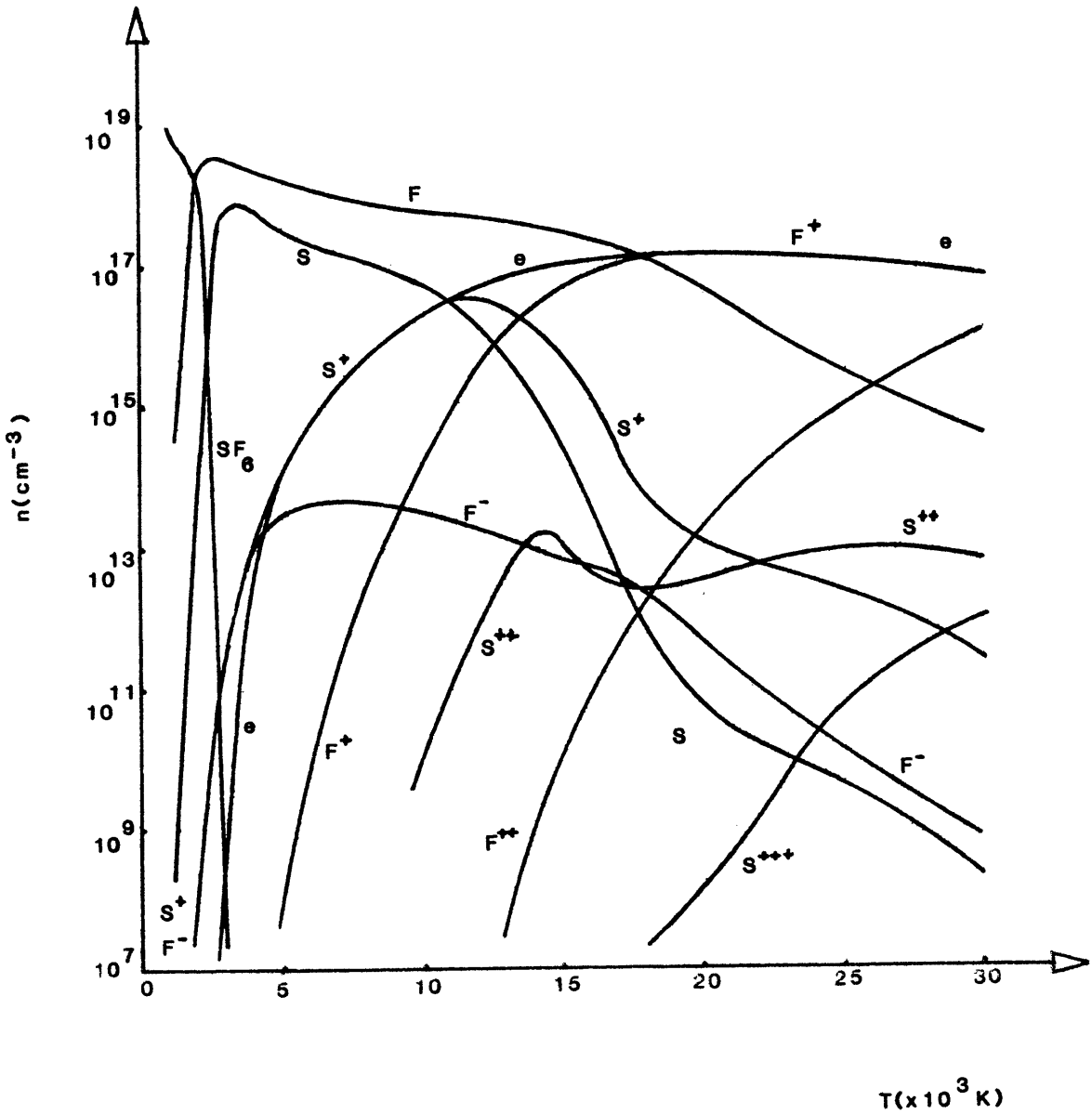

Fig. 1.3.2.(i) Calculated particle number densities as a function of temperature in an SF_6 arc plasma at 1 Atmosphere (after Frie, 1967).

From a knowledge of the particle densities, Frost and Liebermann calculated the electrical and thermal conductivities of the SF_6 plasma using the simplified first approximation of the Chapman-Enskog theory as formulated by Yos (1963) and Brokaw (1960). The electrical conductivity σ was calculated as a function of temperature for pressures of 1, 4, and 16 atmospheres. The curve obtained for 1 atmosphere has been reproduced up to 18000 K in the semilogarithmic plot of Fig. 1.3.2.(ii), and is compared with the corresponding curve for nitrogen at the same pressure, as obtained by Capitelli and Devoto (1973). It can be seen that at lower temperatures the SF_6 plasma has an electrical conductivity greater than that of the nitrogen plasma. This is because the low ionization potential of sulphur allows the production of a large number of electrons at these temperatures in comparison to those produced in the nitrogen arc (in which the molecular ionization potential is 15.5 eV). As the temperature rises, the electrical conductivity of the SF_6 plasma increases more slowly than at the lower temperatures, due to the fact that once most of the sulphur atoms have been ionized, the increase in electron concentration is less rapid because of the high ionization potential of fluorine. Since the ionization potential of atomic nitrogen (14.5 eV) is lower than that of fluorine, it is not surprising that the nitrogen plasma attains a larger electrical conductivity at the higher temperatures. Although not shown in Fig. 1.3.2.(ii), the electrical conductivity of SF_6 continues to rapidly collapse below 4500 K. Swarbrick (1967) attributed the fall in σ below temperatures of this order to the attachment of electrons to fluorine atoms. This hypothesis is supported by the fact that the F^- concentration exceeds that of electrons below 4500 K (see Fig. 1.3.2.(i)).

The thermal conductivity, K, has been calculated by Frost and Liebermann for SF_6 arc plasmas at 1, 4 and 16 atmospheres. The curve for 1 atmosphere is reproduced semilogarithmically in Fig. 1.3.2.(iii) for temperatures up to 18000 K, again with the corresponding nitrogen curve (after Capitelli and Devoto, 1973) included for comparison. The thermal conductivity in molecular

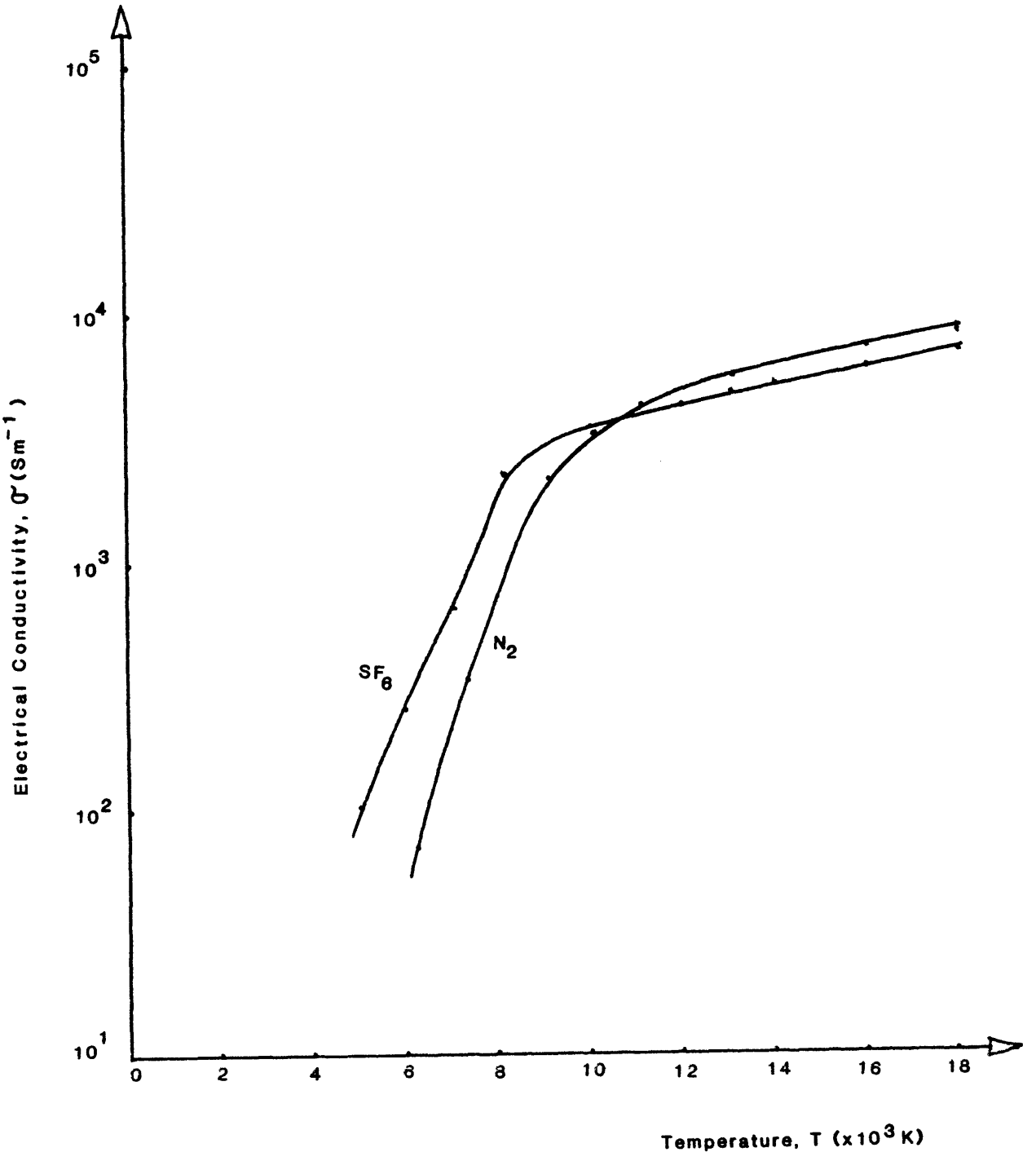

Fig. 1.3.2.(ii) The electrical conductivity of high temperature SF_6 (after Frost and Liebermann, 1971) and nitrogen (after Capitelli and Devoto, 1973) at 1 Atmosphere.

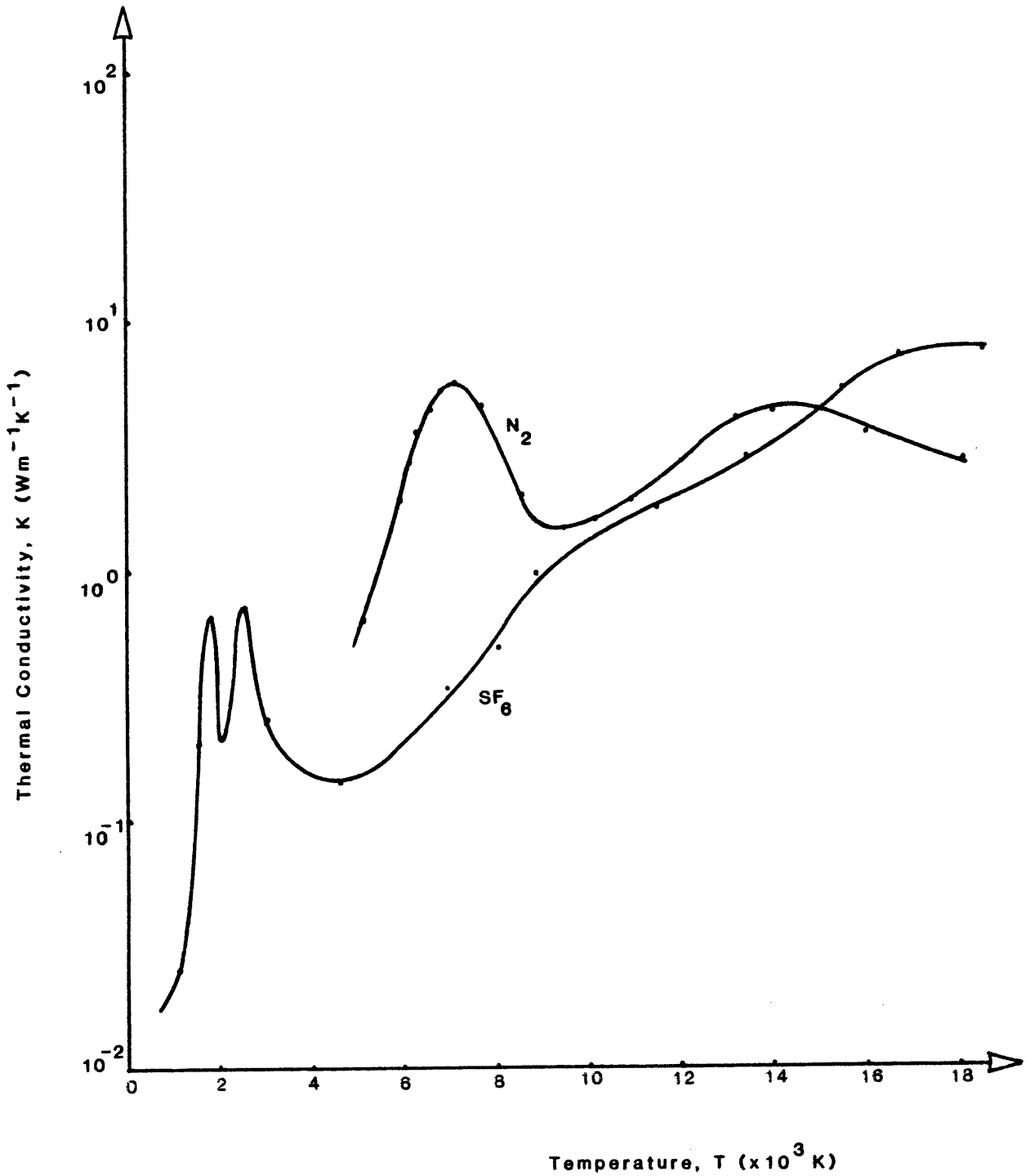

Fig. 1.3.2.(iii) The thermal conductivity of high temperature SF_6 (after Frost and Liebermann, 1971) and nitrogen (after Capitelli and Devoto, 1973) at 1 Atmosphere.

gases is attributable not only to the transport of the kinetic energy of the various species (molecules, atoms, ions and electrons) but also to a number of other processes including for example, the transport of dissociation and ionization energy, and the transport of the internal energies of rotation and vibration. The first of the two sharp peaks in the SF_6 curve of Fig. 1.3.2.(iii) has been shown to be due to the dissociation of the SF_6 molecule, while the second has been attributed to the dissociation of SF_2 and SF_3. It was found that at the temperature corresponding to the first peak (i.e. at 1775 K for one atmosphere), 50% of the neutral SF_6 has dissociated into atomic and molecular fluorine. The data obtained by Frost and Liebermann for this 'half-dissociation' temperature for SF_6 pressures between 1 and 16 atmospheres, can be shown to be given to a good approximation by the empirical relation

$$T = 1775\ (p)^{5.316 \times 10^{-2}} \qquad (1.3.2a),$$

where T is the temperature in Kelvin and p is the pressure in atmospheres. It is not known to what extent equation 1.3.2a holds outside the above pressure range. Nevertheless, if it remains valid for very low pressures, then the half-dissociation temperature at 1 Torr will be 1248 K. The temperature at which thermal dissociation becomes important in SF_6 at pressures less than 5 Torr is of interest in the work to be described later, regarding the low pressure SF_6 spark.

It can be seen from Fig. 1.3.2.(iii) that the thermal conductivity peaks for SF_6 are sharper, and occur at considerably lower temperatures than the nitrogen peak (which occurs around 7000 K). This is because the S-F bond strength of the SF_6 molecule is relatively low (3.9 eV, as determined by Lifshitz *et al.*, 1980) compared to the molecular bond energy of nitrogen (9.76 eV). It can also be seen that over a good portion of the temperature range of Fig. 1.3.2.(iii), the thermal conductivity of the SF_6 plasma is lower than that of nitrogen. The increase in K for both SF_6 and nitrogen at higher temperatures is due essentially to the transport of ionization

energy through ambipolar diffusion, and in SF_6, the positive ion contribution to this energy transport in the temperature range 8000 K to 12000 K is due mainly to S^+ (Swarbrick, 1967).

The electrical and thermal transport properties play a major part in the control of the overall behaviour of an arc plasma. The radial temperature distribution in the arc for example, is critically dependent on the thermal conductivity K, and its variation with temperature (King, 1954). A rough description of this dependence is possible, if it can be assumed that all the energy fed to the arc flows only along an axial core of very narrow cross-section. This is not altogether unreasonable since the electrical conductivity in the outer regions of an arc is known to be small (Swarbrick, 1967). Under the conditions of this assumption, the Elenbaas-Heller energy balance equation (Maecker, 1964b) yields that the radial flow of heat energy is everywhere constant and proportional to $-K\frac{dT}{dr}$ ($\frac{dT}{dr}$ being the radial temperature gradient). Hence for small values of heat conductivity, K, the temperature gradient will be high, while for large values of K, $\frac{dT}{dr}$ will be small.

From these considerations, arcs in SF_6 will in general have higher temperature gradients than those in nitrogen, since the thermal conductivity of SF_6 is for the most part smaller than in nitrogen. Hence for similar axial temperatures, the SF_6 arc will have a smaller cross-section than will the nitrogen arc. When dissociation occurs, the thermal gradients in both gases become quite flat since the thermal conductivities are large. At higher temperatures, where the contribution to heat flow from dissociation has ceased, the thermal conductivity is again low and a steep temperature gradient results, with the formation of a hot core in the arc (King, 1954). In the SF_6 arc at one atmosphere, this core starts to develop just above 2100 K, at which temperature the electrical conductivity is negligible. This means that the current is carried only through the central core since

all other regions will be non-conducting. By contrast, core formation occurs in nitrogen above 7500 K, at which temperature the electrical conductivity is appreciable. Thus the nitrogen core develops at relatively high currents, whereas in SF_6, a central core must always exist, even for very low currents (Swarbrick, 1967).

The properties of SF_6 arcs outlined above, together with the electron attaching properties of the gas, to be discussed in the next Section 1.3.3, combine to make SF_6 an excellent arc-quenching medium in power circuit-breakers. The means by which the above properties facilitate this technical application will be discussed in Section 1.3.4.

1.3.3 Fundamental Electronic Processes in SF_6

In contrast to arc plasmas, description of Townsend and established glow discharges, as well as of the breakdown process itself, requires a fairly detailed understanding of the fundamental electronic processes which occur. This is because in glow discharges, where electrons have a very much higher temperature than the neutral gas molecules, the bulk of energy transfer to the gas is achieved through inelastic electron-molecule collisions (Somerville, 1964). In SF_6 glow discharges, some of the electronic collision processes include, (i) ionization by electron impact, (ii) excitation by electron impact, (iii) electron attachment to neutral molecules and radicals, (iv) electron detachment (both collisional, and by photon impact) from molecules and radicals, (v) electron transfer between negative ions and molecules and (vi), elastic scattering (momentum transfer) between electrons and molecules. One important process not involving electrons is that of molecular and ion-molecule collisions whereby the molecules and ions get rotationally and/or vibrationally excited.

A discussion of some of these processes will now be given in the following section.

1.3.3.(i) Ionization by electron impact in SF_6

The formation of positive ions by electron impact in SF_6 has been studied by Dibeler and Mohler (1948) and Marriott (1954). These workers measured the appearance potentials and relative abundances of the various species using electron beam techniques with mass spectrometric ion detection. At least ten different types of positive ions were found in SF_6 by Dibeler and Mohler when the gas was subjected to the impact of 70 eV electrons. Some of these ions together with their relative abundances (in brackets) are:- SF_5^+ (100), SF_4^+ (10), SF_3^+ (22), SF_2^+ (3.2), SF^+ (4.1), F^+ (0.7). No SF_6^+ ions were observed. Independent experiments by Dibeler and Walker (1966) and by Sasanuma *et al.* (1979) who studied photoionization processes in SF_6, confirmed that the formation of SF_6^+ is negligible in comparison to SF_5^+, SF_4^+ and SF_3^+. Fehsenfeld (1970) who observed the reaction of numerous positive ions (such as He^+, N^+, O^+ etc.) with SF_6 never found SF_6^+ as a product but instead mainly SF_5^+ and some SF_4^+ and SF_3^+. The high relative abundance of SF_5^+ indicates that the dominant (electron impact) ionization process in SF_6 must be given by (Ahearn and Hannay, 1953)

$$e + SF_6 \rightarrow (SF_6^+)^* + 2e \rightarrow SF_5^+ + F + 2e \qquad (1.3.3a).$$

Here the SF_6^+ ion is initially formed in an excited state, but is not stable against decomposition into SF_5^+ and F. The electron beam energy at which this reaction occurs (i.e. the appearance or onset potential of SF_5^+) was found by Dibeler and Mohler to be 15.9 eV, whilst the energies required for the onset of SF_4^+, SF_3^+ and F^+ were 18.9 eV, 20.1 eV and 35.8 eV respectively. Since the appearance potential of F^+ exceeds the energy required for complete dissociation of the SF_6 molecule (D_0 (S - 6F) = 22.4 eV), Dibeler and Mohler suggested that the F^+ ion only results when complete dissociation occurs. The mechanism

$$e + SF_6 \rightarrow (SF_6^+)^* \rightarrow S + 5F + F^+ + e \qquad (1.3.3b),$$

would require 41 eV (since the ionization potential of F is 18.6 eV). However, the mechanism

$$e + SF_6 \rightarrow (SF_6^+)^* \rightarrow S + 4F + F^- + F^+ \qquad (1.3.3c)$$

requires 41 eV - 3.4 eV = 37.6 eV (the 'electron affinity' of the F atom is 3.4 eV and is the amount the energy released by the atom in accepting an electron of zero kinetic energy). Since the energy for this reaction is in reasonable agreement with that for the onset of F^+, Dibeler and Mohler inferred that the onset of F^+ would be accompanied by the production of F^-. This is supported by the sudden increase in the F^- ion current in the experiments of Ahearn and Hannay (1953) at around 34.3 eV (see below).

1.3.3.(ii) Negative-ion formation in SF_6

The ability for a variety of negative ions to form in SF_6 over a wide electron energy range has been a well established fact for nearly 30 years. The numerous possible electron capture processes have been studied by several workers in low pressure (single-collision) experiments using pseudo-monoenergetic electron beams, the pioneers being Ahearn and Hannay, 1953, Marriott and Craggs, 1956 and Hickam and Fox, 1956. From these studies, estimates have been made of the attachment cross-sections for the various negative ion species. Ahearn and Hannay used a mass spectrometer to identify a variety of negative ions such as SF_6^-, SF_5^-, F^- and F_2^- in a low pressure ($< 10^{-5}$Torr) ionization chamber containing SF_6. They studied negative ion currents as a function of electron energy and found that both SF_6^- and SF_5^- currents maximize at less than 2 eV. More recently, Kline *et al.* (1979) measured absolute cross-sections (at room temperature) for SF_6^-, SF_5^-, SF_4^-, SF_3^-, SF_2^-, F_2^- and F^- in the electron energy range, 0-15 eV. Use was made of the 'Retarding Potential Difference' (RPD) method of Hickam and Fox to produce electron beams of 80-100 meV energy resolution. Over the range 2-13eV, the F^- ion is found to have the largest cross-section averaging about

1×10^{-18} cm^2. A broad peak in the SF_5^- cross-section is found to be centred at 0.38 eV, having a magnitude of 4×10^{-16} cm^2. At very low energies (< 0.2 eV) electron capture is observed to lead to only SF_6^- and SF_5^-. The peaks in both of these occur at essentially zero electron energy and are in fact very narrow, their true widths being unknown due to problems associated with the production of true electron beams at such low energies. Above 0.1 eV however, the SF_6^- cross-section has been shown to decrease exponentially with increasing energy (Chantry and Chen, 1976). The magnitude of the SF_6^- cross-section peak at close to zero electron energy has been measured to be 7.0×10^{-14} cm^2 by Kline *et al.* This value was obtained after correcting for the attenuation of the detected SF_6^- signal due to autodetachment of excited SF_6^- ions occurring under the very low pressure conditions used (the phenomenon of autodetachment will be briefly discussed presently). The zero energy peak in SF_5^- is much smaller than the corresponding SF_6^- peak and is of the same order of magnitude as the broad SF_5^- peak occurring at 0.38 eV.

The relatively large attachment cross-sections obtained for SF_6^- and SF_5^- at near-zero electron energy cannot be explained by radiative capture, since the cross-sections for such a process would in general, be some four to six orders of magnitude smaller (Hickam and Fox, 1956). Instead, the large zero-energy peaks are associated with resonance-capture processes (Ahearn and Hannay, *loc. cit.*) of the type represented by

$$e + SF_6 \rightleftarrows (SF_6^-)^* \begin{cases} \rightarrow SF_6^- & (1.3.3d) \\ \rightarrow SF_5^- + F & (1.3.3e). \end{cases}$$

Here, when the electron becomes attached to the SF_6 molecule, the energy liberated in the process goes into increasing the potential (internal)-energy of the negative ion, giving the vibrationally excited state, $(SF_6^-)^*$. The liberated energy is shared between the many degrees of freedom (i.e. among the several modes of vibration and/or rotation) of the molecule, and on the average, a considerable time elapses before this energy is concentrated into a mode which would lead to either a spontaneous ejection of the electron

(autodetachment) or dissociative attachment. Edelson, Griffiths and McAfee (1962) first examined long-lived negative ions using a "time-of-flight" technique (see Massey, 1976), and showed that the SF_6^- ion was metastable and subject to autodetachment, with a lifetime of 10 μs. Compton, Christophorou *et al.* (1966) using much the same technique, obtained a mean lifetime for $(SF_6^-)^*$ of 25 μs. However, Henis and Mabie (1970) obtained a much higher value of > 500 μs, using an ion cyclotron resonance technique (see Massey, 1976). A probable explanation for this large discrepancy is forthcoming from the experiments of Odom *et al.* (1974), whose results suggest that the $(SF_6^-)^*$ ion may be produced in a number of different initial states which differ in lifetime over a wide range. Before autodetachment or dissociative attachment can occur, the excited negative ion may be stabilized to form SF_6^- by collision with neutral molecules. This can occur according to either of the reactions,

$$(SF_6^-)_\nu^* + (SF_6)_0 \rightarrow (SF_6^-)_0 + (SF_6)_\nu \qquad (1.3.3f)$$

$$(SF_6^-)_\nu^* + (SF_6)_0 \rightarrow (SF_6)_\nu + (SF_6^-)_0 \qquad (1.3.3g).$$

Here, the subscripts refer to the excited or zero-order vibrational states. McAfee and Edelson (1963) have suggested that in view of the considerable probability for charge transfer in SF_6, the latter reaction should predominate. Compton *et al.* (1971) have calculated the average time between molecular collisions to be approximately equal to the mean lifetime against autodetachment (taken to be 25 μs) for pressures of the order of 0.1 Torr. This is in support of the findings of Fehsenfeld (1970) who showed from flowing afterglow experiments that the collision-stabilizing reaction is likely to be saturated at pressures in excess of 0.1 Torr. Therefore autodetachment in SF_6 can be assumed to decrease in importance with increasing pressure, above 0.1 Torr.

The dissociative attachment process given by reaction 1.3.3e, occurs at zero electron energy in preference to that by which the products F^- and SF_5 are formed from $(SF_6^-)^*$. This is because reaction 1.3.3e possesses the

lower activation energy (Lifshitz and Weiss, 1972). Neither Lifshitz and Weiss nor Chen and Chantry (1970) have observed F^- by dissociative electron capture from SF_6 at zero electron energy for temperatures below 600 K.

The electron beam studies of Ahearn and Hannay (*loc. cit.*) indicate that the SF_6^- and SF_5^- ion currents fall to very low values following the large peaks at low electron energies, and rise again at electron energies above the onset of SF_5^+ due to secondary electron attachment. Electrons released in reaction 1.3.3a which lie within the critical low energy range will get attached to either an SF_6 molecule or an SF_5 radical. That this secondary electron attachment process occurs, is evidenced by the fact that whereas the primary negative ion currents for electron energies less than 1 eV, are linearly proportional to the gas pressure, the SF_6^- and SF_5^- ion currents much above 1 eV are proportional to the square of the gas pressure. This can be understood from the fact that the probability of capture depends on the product of electron density and gas density and that the number of low speed electrons available for secondary resonance capture is linearly proportional to the gas density. The F^- ion current shows several capture peaks at electron energies greater than 5 eV due probably to a sequence of processes thus:

$$e + SF_6 \rightarrow SF_5 + F^- \qquad (1.3.3h)$$

and

$$e + SF_6 \rightarrow SF_4 + F + F^- \qquad (1.3.3i)$$

etc. The small increase in the F^- current at 34.3 eV has already been discussed in connection with the onset of F^- through the ionization mechanism of reaction 1.3.3c.

Although not observed by Ahearn and Hannay, the negative ion radicals, SF_4^-, SF_3^- and SF_2^- have been accounted for by Kline *et al.* (1979) by dissociative capture processes similar to reaction 1.3.3e:

$$e + SF_6 \rightarrow (SF_6^-)^* \rightarrow SF_4^- + F + F \qquad (1.3.3j)$$

$$\rightarrow SF_3^- + 3F \qquad (1.3.3k)$$

$$\rightarrow \text{etc.}$$

The effect of gas temperature (in the range 300 K to 1200 K) on the attachment of low energy electrons (0-1 eV) to SF_6, has been studied by Chen and Chantry (1970) using a pseudo-monoenergetic electron beam and mass analysis. At room temperature, sharp peaks in SF_6^- and SF_5^- ion currents were observed, as already reported, at essentially zero electron energy. Increasing gas temperature however, was observed to cause a rapid increase in the SF_5^- peak and a decrease in the SF_6^- signal. Above 500 K the SF_5^- signal at zero electron energy exceeded the SF_6^- signal. Although the production of F^- at zero electron energy was not detectable below 600 K (in keeping with the observations of Lifshitz and Weiss, 1972), it increased rapidly with temperature. This indicates that the low energy SF_5^- peak might be due to attachment to vibrationally and/or rotationally excited SF_6 (Compton *et al.*, 1971). In contrast to the strong temperature dependence of the ions produced at zero energy however, the broader peak in SF_5^- production at 0.38 eV was found to be essentially independent of gas temperature.

The electron beam studies discussed above, which describe single electron behaviour in SF_6, have been complemented by the study of electron swarm interactions in SF_6, from which the average behaviour of the electrons is predictable. Most of these swarm experiments have been carried out under uniform-field prebreakdown conditions where space-charge distortion effects are minimal. From such experiments, the relative abundances of the different negative-ion species together with the extent to which collisional detachment and charge-transfer processes occur, have been determined as a function of mean electron energy. In addition, such parameters as the Townsend swarm coefficients, negative-ion mobilities, electron drift velocities and characteristic energies, have also been measured as a function of mean electron energy.

The relative abundances of different negative ion species produced by electron swarm interactions with SF_6 at room temperature have been studied as a function of the parameter E/N (the axial electric field-to-gas number density ratio) by Compton *et al.* (1971) and by McGeehan *et al.* (1975). The parameter E/N governs the mean electron energy of the swarm, and is conveniently expressed in units of "Townsends" where 1 Townsend (1 "Td.") = 1×10^{-17} Vcm^2.

The research groups of Compton and McGeehan used, respectively, front and back illuminated palladium-coated cathodes as a source of photoelectrons in their swarm chambers, and analysed the negative ion species through an orifice in the chamber anodes using mass spectrometry. McGeehan *et al.*, initially using a uniform-field Townsend swarm-chamber, later incorporated a fine wire grid between cathode and anode, as a third electrode. The resulting "double-chamber" was used to reveal the nature of various collision processes, as discussed below. Compton *et al.* and McGeehan *et al.* show that at low pressures ($\sim$ 1 Torr) and low E/N ($< \sim$ 180 Td.) in SF_6, the SF_6^- ions represent some 95% of the total ion current, with about 5%, SF_5^-. Hence the branching ratio in the primary attachment reaction (1.3.3d, and e) is about 20:1 in favour of SF_6^-, at the low pressures referred to. McGeehan's results show negligible pressure dependence of this ratio over the pressure range considered ($\sim$ 1-25 Torr), for E/N < 180 Td. However, at higher E/N, not only is the SF_6^-/SF_5^- ratio lower for a fixed pressure, but also there is an increasing pressure dependence. For example, for E/N = 270 Td., the ratio is approximately 2:1 at 1.0 Torr, but 3:100 at 10 Torr. In addition to this pressure dependence, a significant temperature dependence is observed in the branching ratio, by Fehsenfeld (1970), who worked with a flowing afterglow in SF_6. He found that whilst at 473 K the branching ratio was the same as observed by McGeehan's and Compton's groups for E/N < 180 Td., it had fallen to 9:1 at 530 K (i.e. 10% of the primary attachment reactions were leading to the formation of SF_5^- at this temperature). The relative

abundances of SF_6^-, SF_5^- and F^- obtained by McGeehan *et al.* at room temperature and over a range of E/N from 0 to 450 Td., are reproduced in Fig. 1.3.3.(i). These were obtained under prebreakdown conditions in the original (single) chamber of gap length 4.04 cm and 1.09 Torr pressure. It can be seen from this figure that at E/N of the order of 180 Td., the SF_6^- concentration starts to decline whilst the SF_5^- concentration increases sharply. The mechanism causing this was explained by McGeehan's group following investigations with the double swarm chamber whereby it was possible to selectively inject either SF_6^- or SF_5^- from the first chamber into the second by controlling the E/N parameter in the first chamber (E_1/N). By doing this, it was possible to separately observe reactions involving either one or the other of these species with neutral SF_6 molecules as a function of E/N in the second chamber (E_2/N). By maintaining E_1/N at 90 Td., more than 95% of the total ion current entering the second "reaction" chamber comprised of SF_6^-. Under these conditions, it was observed that when E_2/N reached $\sim$ 180 Td. the SF_6^- concentration in the reaction chamber started to fall away significantly whilst the SF_5^- concentration increased rapidly. McGeehan *et al.* thus interpreted this observation (and hence that made in the single chamber at E/N $\sim$ 180 Td.) as being due to the dissociative charge transfer reaction

$$SF_6^- + SF_6 \rightarrow SF_5^- + F + SF_6 \qquad (1.3.31).$$

The increase in SF_5^- at 180 Td. could not have been due to electronic impact of neutral SF_6 in the reaction chamber because, as shown by O'Neill and Craggs (1973) who used the same apparatus (with E_1/N = 92.7 Td. and $N = 8.1 \times 10^{16}$ cm^{-3}), (a) nearly all photoelectrons produced at the cathode of the first chamber become attached before reaching the grid separating the two chambers and (b) collisional detachment of SF_6^- in the reaction chamber is negligible for all E/N < 460 Td. (This aspect will be discussed later). Hence free electrons could have been present only to a negligible extent.

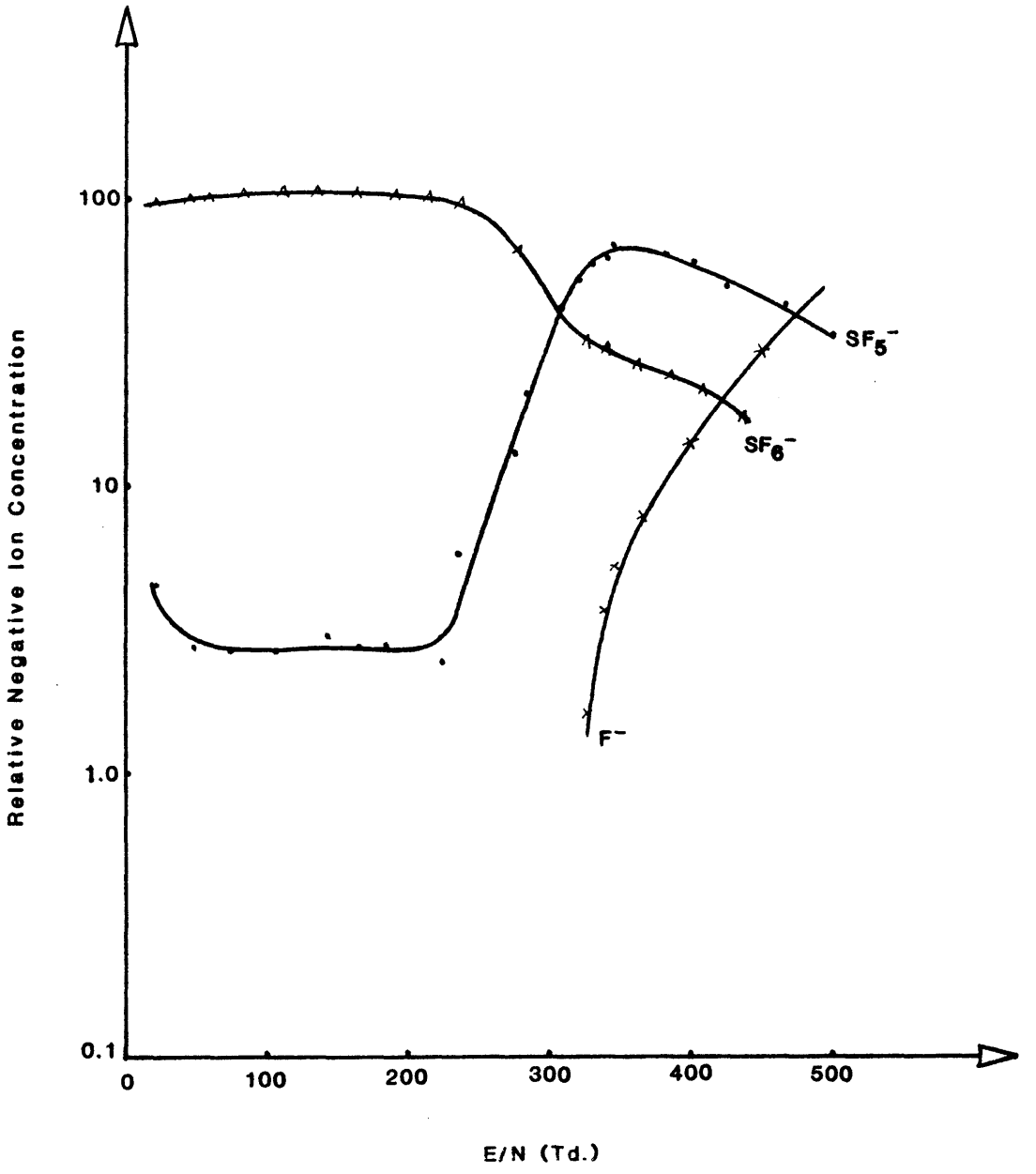

Fig. 1.3.3.(i) Relative negative ion concentrations in SF_6 as a function of E/N at room temperature (after McGeehan *et al.*, 1975).

By increasing E_1/N to a value of 290 Td. at a chamber pressure of 6.35 Torr, McGeehan *et al.* were able to study processes involving SF_5^- since, under the specified conditions, the SF_5^- comprised over 85% of the total ion flow into the reaction chamber. It was observed that for low E_2/N (in this particular experiment, for $E_2/N < 250$ Td.) the SF_5^- ion current sampled in the mass spectrometer formed about 95% of the total with SF_6^- constituting less than 5%. At $E_2/N < 250$ Td. however, the SF_5^- ion current was observed to fall away while the F^- current increased sharply. The mechanism for the general increase in F^- as observed in Fig. 1.3.3.(i) was thus suggested to be

$$SF_5^- + SF_6 \rightarrow F^- + SF_4 + SF_6 \qquad (1.3.3m)$$

or

$$SF_5^- + SF_6 \rightarrow F^- + SF_5 + SF_5 \qquad (1.3.3n).$$

The fall-off in the SF_6^- concentration (as seen in Fig. 1.3.3.(i)) at $E/N > 360$ Td. is prevented in part by the primary attachment process, 1.3.3d, since there are more free electrons at these E/N due to current growth. At higher chamber pressures, the SF_6^- ion current is actually observed to start rising again at $E/N < 300$ Td. McGeehan *et al.* suggested that this might be due to the charge-transfer process

$$F^- + SF_6 \rightarrow SF_6^- + F \qquad (1.3.3o),$$

since the number of free electrons at these E/N was still not high enough to fully account for the observed increase in SF_6^-. Unfortunately, no information appears to be available yet on the cross-sections for these ion-molecule reactions and their energy dependence, which would have made it possible to calculate the rate coefficients for each process as a function of E/N. This information would then have allowed the feasibility of the proposed ion-molecule reactions to be checked. Such information would be particularly useful to check reaction 1.3.3o, which has been observed by Lifshitz *et al.* (1973) to occur on a negligible scale at room temperature, in comparison with the dissociative electron transfer process,

$$F^- + SF_6 \rightarrow SF_5^- + 2F \qquad (1.3.3_p).$$

In keeping with the low pressure, prebreakdown findings of McGeehan's group, Compton *et al.* (*loc. cit.*) found that at $E/p_{20°C} \sim 100$ V Torr^{-1} cm^{-1} ($E/N \sim 300$ Td.), SF_5^- had the same abundance as SF_6^-. At higher E/N, however, poorer agreement was obtained between the findings of the two groups. Whilst McGeehan *et al.* found that F^- became the most dominant negative ion at 500 Td., Compton and co-workers found that this only occurred at $E/p > 400$ V Torr^{-1} cm^{-1} ($\sim$ 1200 Td.), for similar pressure conditions ($\sim$ 1 Torr). Compton's group also observed that at high E/N, as the electron swarm approached discharge conditions, a faint trace of the cluster ion SF_7^- (possibly $F^-(SF_6)$) was observed, whilst under actual discharge conditions, this ion increased greatly in intensity. Unfortunately, no relative abundances of F^-, SF_5^-, SF_6^- and SF_7^- were reported by Compton *et al.* for post-breakdown discharge conditions. They suggested that cluster ion formation might have been enhanced under actual discharge conditions due, in some way, to the increased number of vibrationally excited neutral SF_6 molecules present (due to the increased thermal agitation). Patterson (1969), has also reported the formation of the cluster ions $SF_6^-(SF_6)$, $SF_6^-(SF_6)_2$ and $SF_5^-(SF_6)$ in considerable numbers at low E/N in a drift-tube in which the original SF_6^- and SF_5^- ions were formed in a pulsed spark discharge. Naidu and Prasad (1970) have also reported the cluster ions $SF_6^-(SF_6)$ and/or $SF_5^-(SF_6)$ at $E/p_{20°C} < 60$ V Torr^{-1} cm^{-1} ($E/N < 180$ Td.), but in contrast to Patterson's findings, these were only a few per cent of the total negative ion content (SF_6^- being the dominant species). This difference in relative abundance of cluster ions and SF_6^- was attributed to the different source of initiatory electrons; Naidu and Prasad producing these by back illumination of the cathode.

1.3.3.(iii) Electron detachment in SF_6

In relation to the amount of research that has been published on electron attachment processes in SF_6, comparatively little information is

available on the reverse process of electron detachment. Schlumbohm (1962) demonstrated the occurrence of detachment in SF_6 using an avalanche/drift-tube technique,but made no quantative measurements. Among the first such measurements are those made by Ghosh *et al.* (1967) who determined the ratio of the detachment-to-attachment rate coefficient for SF_6 using a nitrogen afterglow flow system seeded with varying concentrations of SF_6. From the previously determined value of the (two-body) attachment rate-coefficient for thermal electrons in SF_6 (3.1×10^{-7} $cm^3 s^{-1}$, as measured by Mahan and Young, 1966), Ghosh *et al.* obtained a value of 6.2×10^{-13} $cm^3 s^{-1}$ for the SF_6 detachment rate coefficient.

Studies of collision-induced detachment in SF_6 have been made by Eccles *et al.* (1967) and more recently by O'Neill and Craggs (1973). The latter used a double uniform-field ionization chamber, identical in principle to that used by McGeehan *et al.* (1975) who studied attachment and ion-molecule reactions (see Section 1.3.3.(ii)). Using this apparatus, the negative ion species entering the reaction chamber were controlled as already discussed in Section 1.3.3.(ii) by altering the parameter E_1/N (the field-to-gas density ratio in the first (attachment) chamber). O'Neill and Craggs performed spatial current growth studies in the second, variable-gap reaction chamber for different values of E/N in that chamber, (E_2/N). They found that when E_1/N was set at 93 Td. (i.e. so that around 95% of the negative ions entering the reaction gap were SF_6^-), the amplitude of the current growth curves for any fixed N, d_2 and E_2/N was always larger than that obtained when E_1/N was set to 278 Td. (i.e. when the negative ion species entering the reaction chamber were predominantly (> 80%) SF_5^-). This result was taken to imply that detachment from SF_6^- is relatively more pronounced than from SF_5^- and F^-. An overall detachment coefficient, δ/N (without reference to any particular negative ion species) was derived by O'Neill and Craggs using the current growth data in conjunction with a detachment equation given by Eccles *et al.* (1970). Here, δ is the average number of detaching collisions

per negative ion per cm drift in the direction of the electric field. It was found that when E_1/N was held at 93 Td., δ/N decreased with increasing gas density over the range 8×10^{16} cm$^{-3} \leqslant N \leqslant 65 \times 10^{16}$ cm^{-3} for any fixed value of E_2/N used. This trend was also observed in the SF_6 work of Eccles (1968) and in studies of collisional detachment in oxygen by Prasad and Craggs (1965) and Brabenec and Williams (1972). No specific explanation has been presented for the phenomenon. It is unlikely however, that it is due even in part, to the decreasing autodetachment rate in SF_6 at higher pressures, since the bulk of the metastable SF_6^- (i.e. $(SF_6^-)^*$) in the attaching chamber must already have been collision-stabilized at the pressures used (> 2.5 Torr), before entering the reaction chamber (see Section 1.3.3.(ii)).

O'Neill and Craggs found the absolute magnitude of the SF_6 detachment coefficient δ/N at an E/N of 400 Td. and a gas density of 16.2×10^{16} cm^{-3}, to be approximately 2×10^{-19} cm^2. This is over a hundred times smaller than the attachment coefficient η/N, for similar conditions (see Section 1.3.3.(iv) and also Kline *et al.*, 1979, who obtained the attachment coefficient η/N to be $\sim 3 \times 10^{-17}$ cm^2 for the same E/N and for gas densities in the range 3.5×10^{16} cm$^{-3} \leqslant N \leqslant 88 \times 10^{16}$ cm^{-3}). The measured detachment coefficients were inferred to be due predominantly to collisional detachment from SF_6^-, since good fits to the current growth curves were obtained numerically by only considering the detachment reaction

$$SF_6^- + SF_6 \rightarrow 2SF_6 + e \qquad (1.3.3q).$$

This tends to confirm the earlier conclusion that the detachment rates of SF_5^- and F^- are smaller than that of SF_6^- under the specified experimental conditions.

O'Neill and Craggs found that collisional detachment was negligible for the whole range of E/N studied (up to 464 Td.) and concluded that it could be neglected in pre-breakdown current growth studies carried out at these E/N values. They accepted that for higher E/N however, this may cease to be the case.

In the post-breakdown regime, other forms of detachment such as photodetachment, might contribute to the overall value of δ/N. Photodetachment cross-section studies in SF_6 do not appear to have been reported in the literature as yet. Information however, is available on the photodetachment of negative atomic fluorine ions, which, as has already been shown, is the dominant negative ion species in SF_6 at high E/N (> 475 Td.).

Berry and Reimann (1963) measured photodetachment thresholds of the fluorine negative ion by studying its absorption spectrum in shock-heated vapours of CsF, RbF and KF salts. The spectrum obtained was a continuum with two sharp thresholds at 3595 $\mathring{A}$ and 3542 $\mathring{A}$. These thresholds were respectively assigned, on the basis of their separation and relative intensities to the onset of the photodetachment processes,

$$F^-(^1S_0) + h\nu \rightarrow F(^2P_{3/2}) + e \qquad (1.3.3r)$$

and

$$F^-(^1S_0) + h\nu \rightarrow F(^2P_{1/2}) + e \qquad (1.3.3s).$$

The experimental cross-sections for these processes were found to be 2.5 ± 2 x 10^{-18} cm^2 and 0.8 ± 0.4 x 10^{-18} cm^2 for 1.3.3r and 1.3.3s, respectively, at wavelengths 20 $\mathring{A}$ below the corresponding thresholds. A total experimental cross-section of 3.3 ± 2 x 10^{-18} cm^2 was obtained at an energy of 0.07 eV above the low energy threshold (corresponding to 3595 $\mathring{A}$). From this threshold the electron affinity of atomic fluorine was determined by Berry and Reimann to be 3.448 ± 0.005 eV. It should be noted that for negative atomic ions, such as F^-, the electron affinity is also the energy required to detach the least tightly bound electron from the ion, i.e. the electron affinity is equal to the minimum detachment energy (for molecules, however, the electron affinity and detachment energy are not simply related; this will be discussed shortly).

Absolute photodetachment cross-sections of F^- have been measured over a photon energy range between 3.4 eV and 5.88 eV by Mandl (1971), using a technique similar to that of Berry and Reimann. Fig. 1.3.(ii) shows Mandl's

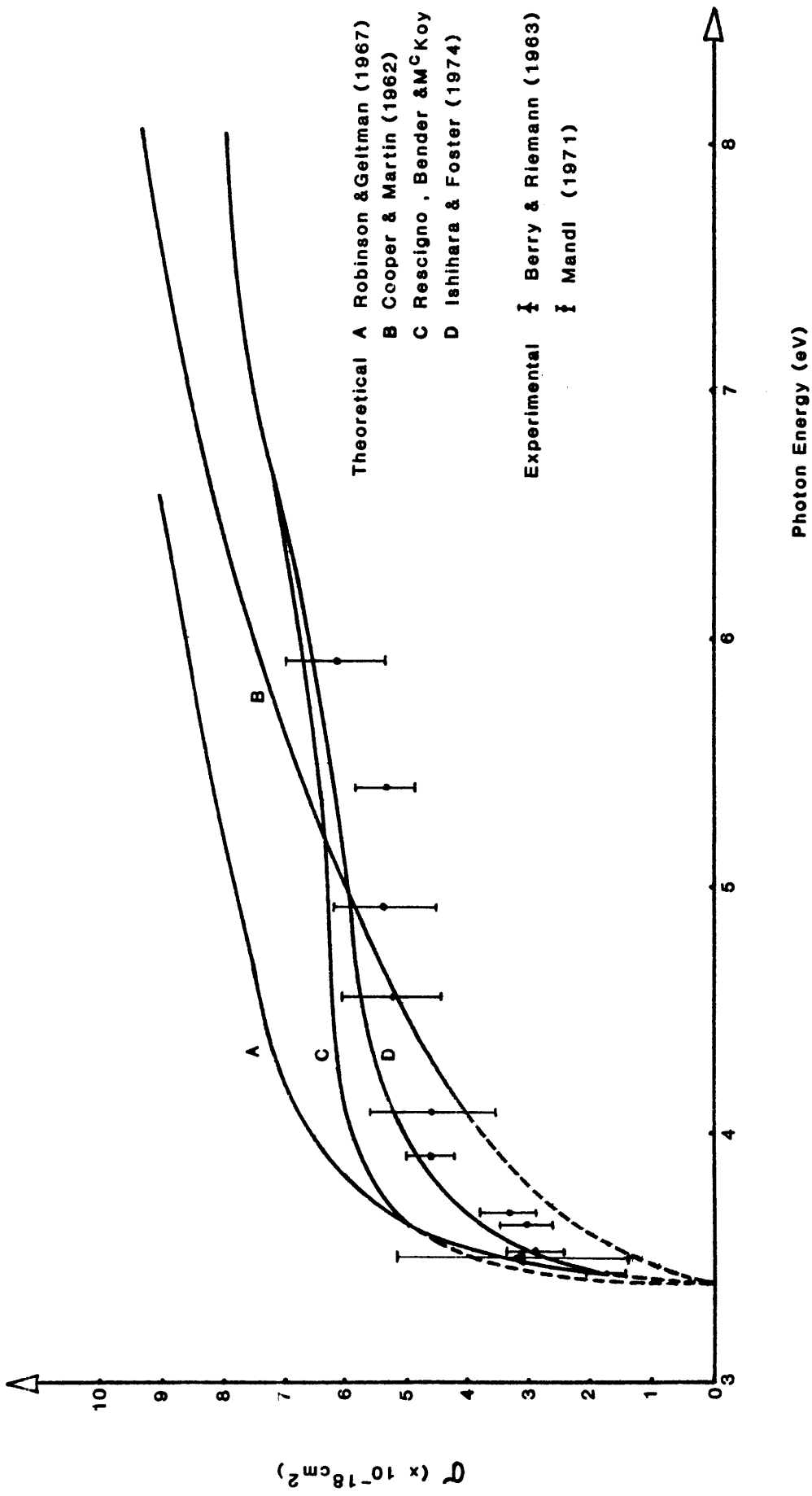

Fig. 1.3.3.(ii) The photodetachment cross-section of F^- as a function of photon energy, as determined by several workers, from both theory and experiment.

results together with the single cross-section measurement of Berry and Reimann. Also shown in this figure are calculated cross-sections obtained by Cooper and Martin (1962), Robinson and Geltman (1967), Ishihara and Foster (1974) and Rescigno, Bender and McKoy (1978). These calculated cross-sections were derived using a variety of theoretical methods. It can be seen that apart from the results of Cooper and Martin, the cross-sections rise sharply as a function of photon energy from the threshold. Hotop and Lineberger (1975) made very accurate measurements of relative photodetachment cross-sections in this threshold regime by observing the absorption of radiation from a tunable dye laser of high frequency resolution, in a beam of F^- ions. From these measurements, the thresholds corresponding to the onset of the photodetachment processes described by Berry and Reimann, could be determined to a high degree of precision. From their measured threshold for the process given by 1.3.3r, Hotop and Lineberger obtained the electron affinity of atomic fluorine (i.e. its minimum detachment energy) to be 3.399 ± 0.003 eV, in contrast to the higher (and less accurate) value obtained by Berry and Reimann.

No accurate measurements have yet been made of the detachment energies of SF_6^- and SF_5^-. As mentioned earlier, the detachment energy of a negative molecular ion is not simply related to the electron affinity, as it is with negative atomic ions. The electron affinity of a molecule is defined as the difference in the energies of the neutral molecule and its molecular ion when both structures are in their normal electronic and nuclear states, the affinity being positive when the neutral molecule has the larger energy (McDaniel, 1964). This energy is equal to the electron detachment energy only if a transition between normal states is involved. In general, the molecular ion potential curve will have its minimum at a different internuclear separation compared to the minimum of the neutral molecule potential curve. According to the Franck-Condon principle, transitions from the normal state of the negative molecular ion to the ground electronic state of the

molecule, will occur without a change in nuclear separation. The energy required for this is called the *vertical* detachment energy, and in general is different to the electron affinity. Nevertheless, a knowledge of the electron affinities of SF_6 and SF_5 together with other relevant thermodynamic data makes it possible to deduce approximate upper limits for the vertical detachment energies of SF_6^- and SF_5^-.

The electron affinity of SF_6 has been evaluated by Lifshitz *et al.* (1973), from measurements of the translational-energy threshold for electron transfer to SF_6, from atomic negative ions such as S^- and O^-. A mean value of 0.63 eV was obtained for the electron affinity of SF_6 from these measurements. Lifshitz and his co-workers evaluated the electron affinity of SF_5^- from the measured threshold energy for the dissociative charge transfer reaction,

$$X^- + SF_6 \rightarrow SF_5^- + F + X \qquad (1.3.3t).$$

Here X^- is a suitable atomic negative ion for which the electron affinity is accurately known. The measured threshold energy for this reaction is given by

$$\Delta H = EA(X) + D_0(SF_5 - F) - EA(SF_5) \qquad (1.3.3u),$$

where $EA(X)$, $EA(SF_5)$ are the electron affinities of species X and SF_5 respectively, and $D_0(SF_5 - F)$ is the bond dissociation energy of the SF_6 molecule (i.e. the minimum energy required to break the $(SF_5 - F)$ bond without leaving the products in excited electronic or nuclear states). Equation 1.3.3u will apply provided that the SF_5^- product is formed without excess kinetic or internal energy. Using the new accurate value of 3.9 ± 0.15 eV for $D_0(SF_5 - F)$ as obtained by Kiang *et al.* (1979), together with the appropriate values of $EA(X)$ and ΔH, Lifshitz *et al.* (1980) obtained $EA(SF_5) \geq 3.4 \pm 0.2$ eV.

From their derived thermodynamic data, Lifshitz *et al.* (1973) qualitatively constructed a quasidiatomic potential energy diagram for SF_6 and SF_6^- (assuming that they are both composed of only two particles, i.e. SF_5/SF_5^- and F). From this diagram it is apparent that the vertical detachment energy of SF_6^- cannot exceed the sum of the electron affinity of SF_6 and the bond

dissociation energy of SF_6, i.e. $D_0(SF_5 - F)$. This sum amounts to 4.53 eV. Similarly for SF_5^-, the vertical detachment energy cannot exceed the sum of the electron affinity of SF_5 and the bond dissociation energy of this radical, $D_0(SF_4 - F)$. The latter quantity has been evaluated by Fehsenfeld (1971) to be $\leq$ 1.5 eV, so that the vertical detachment energy of SF_5 must be less than 4.9 eV.

1.3.3.(iv) Important swarm parameters of SF_6

In order to put the study of phenomena in SF_6 discharges on a quantitative basis, a variety of basic data have been obtained on the processes of ionization and attachment and on such parameters as electron drift velocities and electron characteristic energies. One of the fundamental parameters used to describe the behaviour of swarms of electrons travelling through a gas under the influence of an applied electric field is the Townsend primary ionization coefficient, α, which is defined as the number of ionizing collisions made per electron per centimetre in the applied field direction.

In electron attaching gases, current growth is affected by such processes as ionization, attachment, electron-transfer and detachment. Hence a net ionization coefficient, λ, is defined for these gases as $\lambda = \alpha - \eta'$. Here α is the primary ionization coefficient, and η' the effective attachment coefficient, which is a complex function of the individual attachment, detachment and charge-transfer coefficients (Kline *et al.*, 1979). The coefficient η' is defined in exact analogy with the definition of α, and represents the effective number of attachments per electron per centimetre in the field direction. λ/N, α/N, η'/N etc. are the *reduced* Townsend coefficients where N is the gas number density. These coefficients are govered by the mean electron energy which, as already explained in Section 1.3.3.(ii) is directly controlled by the reduced field, E/N. The values of α and η' for SF_6 have been computed by Bhalla and Craggs (1962) from spatial current growth curves, using a careful process of curve-fitting, and employing the

modified Townsend current growth equation derived by Geballe and Reeves (1953). This equation takes into account the effect of electron attachment in prebreakdown current growth, but assumes that such processes as detachment, electron transfer, photoionization and electron losses through radial diffusion are negligible. From the computed values of α and η, Bhalla and Craggs plotted the reduced coefficients α/p, η/p and $\frac{\alpha-\eta}{p}$ as a function of E/p, p being the gas pressure reduced to 20^0C. They found that over the whole range of pressures used (from 5 Torr to 100 Torr) α/p was equal to η/p at an E/p value of 117.5 V $Torr^{-1}$ cm^{-1}. Kline *et al.* (*loc. cit.*) performed similar measurements in SF_6, and found that the net ionization coefficient $\lambda(= \alpha - \eta')$ was equal to zero when E/N was equal to 3.62×10^{-15} Vcm^2(= 362 Td). This value of E/N corresponds to an E/p at 20^0C of 119.5 V $Torr^{-1}$ cm^{-1}, which is in good agreement with Bhalla and Craggs' value. Kline and his collaborators also calculated α/N and η'/N from the electron energy distribution which they computed by numerically solving the Boltzmann equation. To do this a complete set of collision cross-sections was used, including those of momentum transfer, attachment, ionization, and electronic and vibrational excitation. Good agreement was obtained between the measured and calculated values of η'/N over the range of E/N from 300 to 570 Td if the attachment cross-sections were uniformly increased in magnitude by 35%. In the calculation of η'/N it was assumed that detachment is negligible in this E/N range (this is reasonable on the basis of O'Neill and Craggs' findings - see Section 1.3.3.(iii)), and that electron transfer processes create stable negative ions with very small detachment cross-sections. Good agreement was also found between the measured and calculated values of α/N in the above range of E/N when a suitable electronic excitation cross-section was used.

From the electron energy distribution computed by Kline *et al.* for SF_6, the electron drift velocity v and electron 'characteristic energy' D/μ (where D is the free diffusion coefficient for the electrons and μ, the

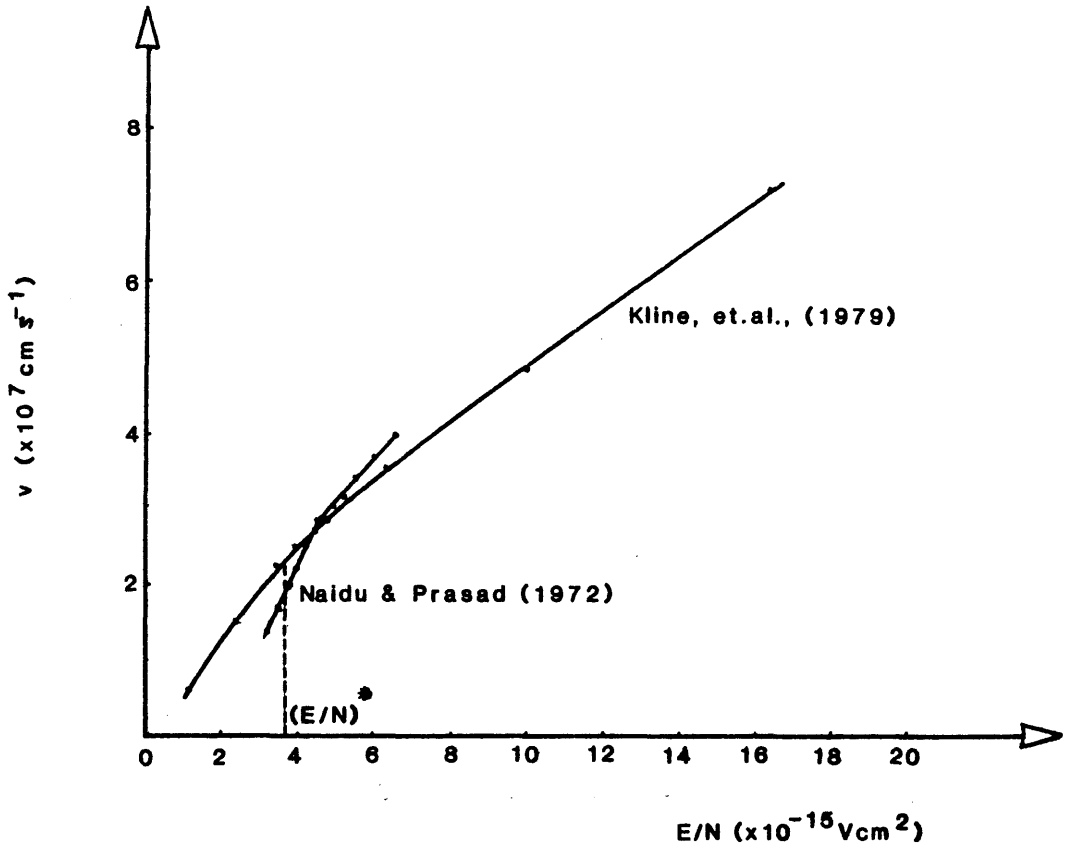

Fig. 1.3.3.(iii) Electron drift velocity (v) in SF_6 as a function of E/N, as calculated by Kline *et al.* (1979) and measured by Naidu and Prasad (1972).

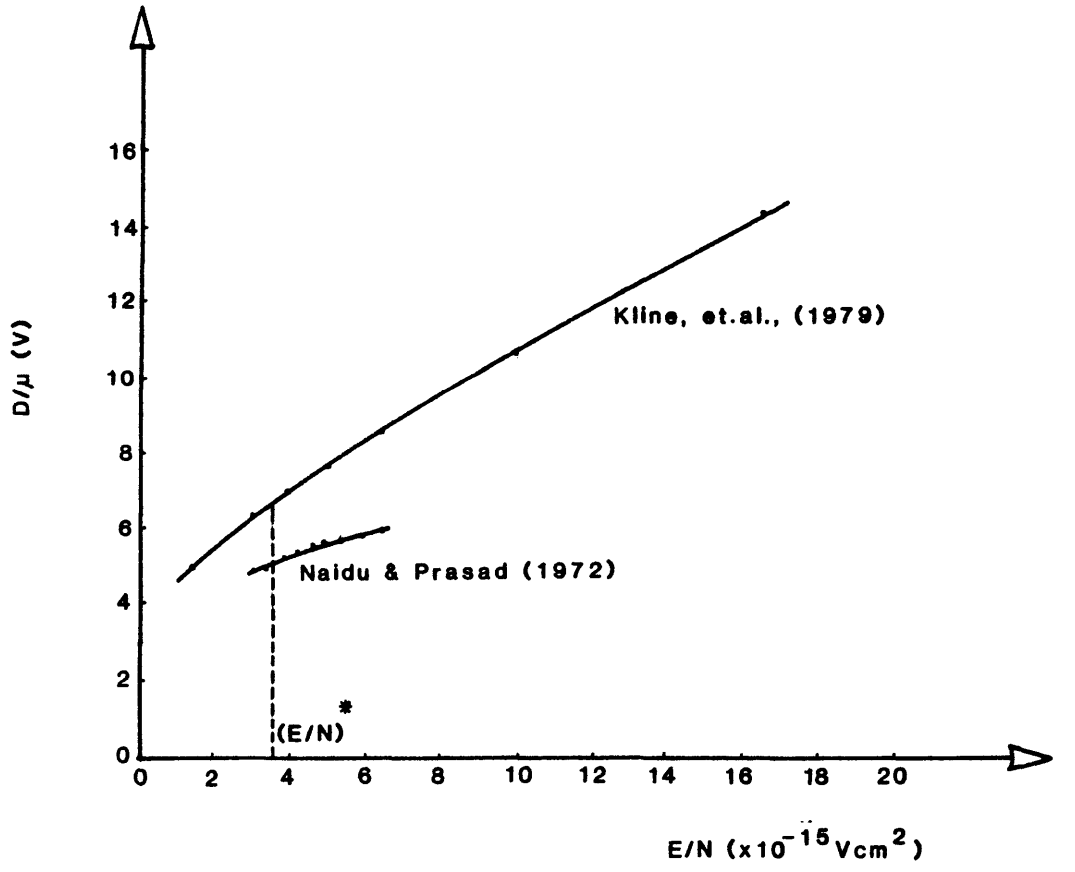

Fig. 1.3.3.(iv) Electron characteristic energy (D/μ) in SF_6 as a function of E/N, as computed by Kline *et al.* (1979) and measured by Naidu and Prasad (1972).

electron mobility) were calculated as a function of E/N over the range 33 to 1700 Td. These results have been reproduced in Fig. 1.3.3.(iii) and (iv) over the range 100 < E/N < 1700 Td and the experimental results due to Naidu and Prasad have been included for comparison. Better agreement exists between the measured and calculated W-curves than between the corresponding D/μ-curves.

A knowledge of the swarm parameter, D/μ, as a function of E/N is very useful, since for a known electron energy distribution, the mean electron energy of the swarm can then be related to the parameter E/N (see McDaniel, 1964 and Meek and Craggs, 1978). The general relationship between the mean electron energy, $\bar{\varepsilon}$ and D/μ is

$$\bar{\varepsilon} = \frac{1}{2} m\overline{c^2} = \frac{e}{F} \cdot \frac{D}{\mu} \qquad (1.3.3v)$$

where e, m and c are the electronic charge, mass and random velocity respectively, while F is a dimensionless factor lying between 0.5 and 1 (Huxley and Crompton, 1974), the exact value of which depends on the nature of the electron energy distribution. For a Maxwellian distribution, for example, F = 0.67.

Using their calculated electron energy distribution, Kline *et al.* obtained a mean electron energy of $\bar{\varepsilon}$ = 8.7 eV for E/N = $(E/N)^*$ (= 362 Td.). From Fig. 1.3.3.(iv) it can be seen that at this E/N, D/μ = 6.65 volts from the theoretically derived curve, suggesting that for Kline's electron energy distribution, F = 0.76.

These data of D/μ as a function of E/N have particular relevance to an SF_6 glow discharge phenomenon which is discussed in Ch. 3.

1.3.3.(v) Breakdown in SF_6

(a) *Uniform field breakdown*

The threshold condition for uniform field breakdown in electronegative gases was shown by Geballe and Reeves (1953) to be given by the equation

$$\left[\frac{\gamma\alpha}{\alpha-\eta}\right]\left[\exp\{(\alpha-\eta)d\} - 1\right] = 1 \qquad (1.3.3w).$$

Here α and η are the usual primary ionization and attachment coefficients, γ is the probability per positive ion or photon of liberating an electron from the cathode, and d is the gap length. From this equation it was shown that if $\alpha/p \geq \eta/p$, breakdown is possible for sufficiently large pd regardless of the values of α/p, η/p and γ. However, if $\alpha/p < \eta/p$, equation 1.3.3w would approach, with increasing pd, an asymptotic form which is independent of pd, i.e.

$$\alpha/p = \eta/p.\left[\frac{1}{1+\gamma}\right] \qquad (1.3.3x).$$

This equation is a condition on E/p alone and fixes a limit for this parameter denoted by $(E/p)^*$, below which no sparking should be possible regardless of the magnitude of pd. The magnitude of γ is expected in general to be sufficiently small that it can be neglected in equation 1.3.3x. Hence the relation $\alpha/p = \eta/p$ was suggested by Geballe and Reeves as being a working condition for the limiting E/p. This prediction was first tested by Bhalla and Craggs (1962) who measured the uniform field sparking E/p, as a function of pd. They found that as pd is increased, the value of E/p falls away very rapidly at first, then gradually, and eventually approaches a limiting value given by $(E/p)^* = 117.5$ V Torr^{-1}cm^{-1}, below which breakdown does not occur until pd is increased beyond a value which increases with pressure. This decrease in the breakdown E/p below the limiting value has been attributed to a non-uniform field effect (see Section 1.3.3.(v)b). As already discussed in the previous section, Bhalla and Craggs also found that $\alpha/p = \eta/p$ at 117.5 V Torr^{-1} cm^{-1} from their spatial current growth experiments, and so confirmed the theory of Geballe and Reeves. An extension to this theory has been made (Thomas, 1968 - see Meek and Craggs, 1978, Ch. 6), which includes electron transfer and detachment, and which gives the current growth equation of Geballe and Reeves if attachment only is considered.

The breakdown potentials (V_s) in SF_6 were measured by Bhalla and Craggs in the pressure range between 5 and 200 Torr (all pressures corrected to 20^0C) for values of pd up to 400 Torr cm. It was found that the breakdown potentials were substantially higher than for air or nitrogen for corresponding values of pd. Thus for example, at pd = 380 Torr cm, SF_6 has a 'dielectric strength' (breakdown field strength) of 2.8 relative to dry air. The Paschen curve for SF_6 in the range of Nd between 3×10^{17} cm^{-2} and 3.3×10^{18} cm^{-2} has been plotted in Section 3.1.2 (see Fig. 3.1.2.(i)), the data points having been taken from a table published by Dakin *et al.*, 1974 (see Meek and Craggs, 1978, Ch. 6). For Nd $\lesssim$ 50×10^{18} cm^{-2}, the breakdown voltages are the same using stainless steel, aluminium or nickel electrodes, and the effect of cathode irradiation is observed to be small (see also Meek and Craggs, 1978).

(b) *Non-uniform field breakdown (in SF_6)*

The subject of breakdown in non-uniform fields is a vast and complex one. Its study in SF_6 has arisen in part from the fact that most practical discharge devices utilizing this gas, have grossly non-uniform applied electric fields. Further, supposedly uniform-field configurations are sometimes non-uniform and give an apparent deviation from Paschen's law. Studies have thus been made into the cause of such non-uniformities. A detailed review of non-uniform field breakdown is given by Waters (see Meek and Craggs, 1978, Ch. 5).

The quantitative physical analysis of ionization growth in a particular non-uniform field gap, of necessity requires a knowledge of the associated applied electric field distribution. This information is now obtainable by numerical methods using computers. The field configurations that have been studied by these methods include sphere-plane gaps, rod-plane gaps, conductor-plane gaps, sphere-sphere gaps etc. Waters (*loc. cit.*) points out that any account of ionization growth must recognize that the initial field distribution will be grossly modified by the accumulation of space charges produced during spark development, as indeed happens also in so-called uniform field breakdcwn.

A semi-empirical expression for the breakdown criterion on compressed SF_6 has been determined by Pedersen (1970), based on the Meek criterion for streamer growth. By applying to this criterion, the results of computed electric field distributions for a variety of gap configurations, Pedersen calculated the breakdown voltages for these asymmetric gaps. Good agreement was obtained between calculated and measured sparkover voltages for sphere gaps and for concentric and eccentric sphere-hemisphere gaps in SF_6. Semi-empirical equations have also been obtained by several other workers for the breakdown field in SF_6 as a function of gas number density for different types of gap including coaxial cylinder and rod-rod geometries (Meek and Craggs, 1978).

In gaps where the electric field is non-uniform, breakdown is often preceded by a corona discharge, which may take one of several different forms. The study of these various forms of corona constitutes a separate subject and will not be dealt with here (excellent reviews have been presented on corona discharges by (i) Sigmond (Meek and Craggs, 1978, Ch. 4) and (ii) Goldman and Goldman (Hirsh and Oskam, 1978, Ch. 4)). Corona discharges occur when the applied voltage exceeds the corona inception voltage, V_i, which can be considerably lower than the voltage, V_s, required to produce breakdown across the gap. An increase in gas density usually leads to an increase in both V_i and V_s but an important exception to this rule is provided by electronegative gases and mixtures containing electronegative gases. In these special cases, for a fixed gap, an increase in gas density (usually above that corresponding to a few atmospheres) causes the breakdown voltage to pass through a maximum and then fall until at a critical value of density, it has reached the level of the corona inception voltage. The breakdown voltage then increases with density above this critical value, but the breakdown process is no longer preceded by corona (Blair: see Meek and Craggs, 1978, Ch. 5). Such behaviour is observed with static and impulse voltages of both polarities, and alternating voltages. For a given experimental arrangement, the maximum in the

breakdown voltage occurs at higher gas densities when the high voltage electrode is negative, than when it is positive. To account for the negative slope in the V_s against N curve, Works and Dakin (1953) (see Meek and Craggs, 1978, Ch. 5) suggested that at gas densities above that corresponding to the maximum breakdown voltage, corona streamer propagation across the gap is enhanced by reduced positive ion diffusion.

Because of the rather rapid variation in SF_6 of the reduced net ionization coefficient, $\frac{\alpha-\eta'}{N}$ with E/N in the region of $(E/N)^*$ (refer to the work of Kline *et al.*, 1979; Bhalla and Craggs, 1962, as discussed in Section 1.3.3.(iv)), the onset of discharges in this gas at high pd will be determined almost entirely by the maximum field strength in the (asymmetric) gap. For this reason, V_i and V_s are more strongly dependent on the form of the electrodes than in other gases, such as air (Nitta and Shibuya, 1971 - see Meek and Craggs, 1978, Ch. 6). Under non-uniform field gap conditions, discharges in SF_6 appear to be initiated with an applied electric field strength lower than that corresponding to $(E/N)^*$, and therefore under conditions where cumulative ionization is theoretically impossible. An example of this effect (already mentioned in the previous sub-section) is the anomalous breakdown effect observed by Bhalla and Craggs (1962). This has been attributed to local field enhancement at the edges of the profiled uniform-field electrodes (Nielsen and Pedersen, 1972; Davies *et al.*, 1976).

Other factors which can substantially alter the breakdown voltage of a gap are microprotrusions on electrode surfaces, and the presence of solid particles in the gap. Gockenbach (1976) for example has indicated that locally enhanced fields due to sharp points on the electrode surfaces, result in a decrease in breakdown voltage with increasing gas pressure. The dependence of breakdown voltage in SF_6 and SF_6 mixtures, on electrode surface roughness, has been studied by Crichton *et al.* (1976) by considering experimentally and theoretically, the effect of a single protrusion incorporated into one electrode of a uniform field gap. They showed that the "roughness factor", ξ (i.e. the ratio of the breakdown E/p for the system in question, to the

limiting E/P below which breakdown in a strictly uniform field is impossible) decreases rapidly from unity with an increase in the product pR, where p is the gas pressure and R is a characteristic dimension of the protrusion (R includes both the height and the radius of curvature of the protrusion). The results obtained indicate that pure SF_6 is considerably more sensitive to surface roughness than SF_6 mixtures and non-attaching gases.

Numerous workers have studied the effect of solid particles on non-uniform field breakdown in compressed SF_6. Cookson and Farish (1973) for example, applied alternating (50Hz) voltages and 'lightning-impulse' voltages (i.e. high voltage pulses of microsecond rise- and fall-times) to parallel-plane gaps and coaxial-cylinder gaps, and observed the effects of spherical and cylindrical conducting particles both free to move and fixed to an electrode surface. Their results, together with those of other investigators, have shown that the effects of solid particles are both complex and substantial. The breakdown voltage can be reduced to as little as 10% of the value measured in the uncontaminated gas. The mechanism by which the particles affect the breakdown process is not fully understood as yet (Cookson and Farish, 1973).

1.3.4 Some Applications of SF_6

High voltage insulation and switchgear applications

The numerous properties of SF_6 that have been discussed in Sections 1.3.2 and 1.3.3 have made it ideal for use as an insulant in high voltage devices and as the carrier gas for arc discharges in electrical switchgear. At present, the SF_6 gas-blast circuit breaker appears to be one of the most efficient available for very high-voltage circuit-interruption.

The prime requirements of an a.c. circuit-breaker medium is that the arc formed upon contact separation, be capable of being cooled in the current-zero region and the medium being rapidly returned to an insulating state. Following this, its dielectric strength should be high enough to prevent re-striking as the voltage rises.

Circuit-breaker media are often characterised by their thermal time-constant, defined as the time taken to reduce the electrical conductivity of the arc by a factor of $\frac{1}{e}$ due to temperature decay. The rate of temperature decay in modern gas-blast circuit-breakers, depends in a complicated way on mechanisms such as convection, conduction, turbulence and radiation. In the current-zero region, however, the main mechanism of temperature decay appears to be thermal conduction. In molecular gases, the temporal decay of (electrical) conductance is governed not by one, but at least two time constants (see for example, Hertz *et al.* 1971). Nevertheless, Frind (1960) has shown that it is a useful approximation to assume that the electrical conductivity of an arc decays with a single time constant, θ, given by

$$\theta = \frac{\pi r_0^2}{\pi(2.40)^2 k} \qquad (1.3.4a)$$

where πr_0^2 is the area of the conducting portion of the arc and k is the thermal 'diffusivity' of the plasma. Consequently, if k is constant, the narrower the arc channel, the smaller will be the thermal time-constant and the faster will be the electrical conductivity decay as a result of a temperature decrease in the current zero region. Clearly therefore, a small thermal time-constant is a major criterion (Browne, 1948) for successful interruption in circuit breakers.

As described in Section 1.3.2, the current in the SF_6 arc at one atmosphere is carried solely through a narrow central core, above a temperature of 2100 K. This core is much narrower than that formed in nitrogen because (i) in contrast to the SF_6 arc, the nitrogen arc has appreciable electrical conductivity when its core is formed (above 7500 K) and (ii) the thermal conductivity of the SF_6 arc is in general smaller than that of nitrogen. Since the thermal diffusivity of these two gases is similar (Swarbrick, 1967), it follows that the SF_6 arc will have a much smaller time-constant than the nitrogen arc. Below 2000 K in the SF_6 arc, the rate of ionization is quickly reduced due to the loss of free sulphur by recombination with fluorine

(sulphur being the only product of the SF_6 arc which can be ionized below this temperature), and further by the attachment of free electrons to fluorine. It should be noted that the latter process is quite efficient due to its relatively high cross-section ($\sim 10^{-18}$ cm^2) for electron energies from 4 to 12 eV (see Kline *et al.*, 1979). Thus the smaller time-constants of arcs in SF_6 (with respect to nitrogen) make this gas very suitable for the rapid extinction of circuit-breaker arcs in the current-zero region. Furthermore, its high dielectric strength (more than 2.5 times that of nitrogen) resulting from its strongly electronegative properties, allows it to withstand high rates of voltage recovery following current-zero.

Despite its numerous advantages as a circuit breaker medium, SF_6 has the disadvantages of high cost and low liquefaction pressure (22.5 atmospheres at 25^0C - Schumb, 1947). Furthermore, it is well known that the dielectric-strength of this gas is very sensitive to electrode surface roughness, as already discussed in Section 1.3.3.(v)(b), especially at high pressures. In view of these problems, much research is presently being carried out on the feasibility of using SF_6 mixtures as circuit-breaker media. It is known that if a small amount of an electronegative gas such as SF_6 is added to nitrogen or air, a disproportionately large increase in dielectric-strength occurs. For example, the measured value of the limiting E/N in a 50% N_2: 50% SF_6 mixture is about 90% of the limiting E/N-value in pure SF_6 (i.e. the dielectric strength of this mixture is 90% that of pure SF_6 - see Kline *et al.*, 1979). Furthermore, such a mixture costs only about one half that of pure SF_6 at the same pressure. In addition to these advantages, it has been shown (see Section 1.3.3.(v)(b)) that the dielectric-strength of SF_6 mixtures is less sensitive to electrode surface microprotrusions than that of pure SF_6, for certain ranges of the parameter pR. In many ways, therefore, SF_6/N_2 mixtures may be preferable to pure SF_6 as a practical medium for gas-blast circuit-breakers, even more so in view of the higher liquefaction pressures of such mixtures. Numerous other mixtures such as SF_6/N_2O, SF_6/'FC-75' and

SF_6/He are also currently being studied in the search for the best possible combination for high voltage insulation.